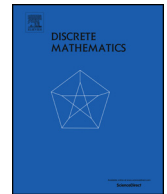




Contents lists available at ScienceDirect

Discrete Mathematics

journal homepage: www.elsevier.com/locate/disc

Structural parameters of Schnyder woods

Christian Ortlieb ^{*,1}, Jens M. Schmidt ¹

Institute of Computer Science, University of Rostock, Germany



ARTICLE INFO

Article history:

Received 2 January 2024

Received in revised form 30 September 2024

Accepted 1 October 2024

Available online xxxx

Keywords:

Schnyder wood

3-connected planar graph

Ordered path partition

Leaf

Singleton

ABSTRACT

We study two fundamental parameters of Schnyder woods by exploiting structurally related methods. First, we prove a new lower bound on the total number of leaves in the three trees of a Schnyder wood. Second, it is well-known that Schnyder woods can be used to find three compatible ordered path partitions. We prove new lower bounds on the number of singletons, i.e. paths that consists of exactly one vertex, in such compatible ordered path partitions. All bounds that we present are tight.

© 2024 The Author(s). Published by Elsevier B.V. This is an open access article under the CC BY license (<http://creativecommons.org/licenses/by/4.0/>).

1. Introduction

We are interested in gaining more insights into the structure of 3-connected planar graphs. It is well-known that these graphs admit Schnyder woods, which have many applications and implications for planarity and graph drawing, see for example [1–4,8–10,16,18–20]. We study two fundamental parameters of Schnyder woods, namely the number of leaves and the number of singletons, and provide new lower bounds for them. We also give a characterization of the minimal element of the Schnyder wood lattice that allows for easy verification.

Schnyder woods and ordered path partitions A Schnyder wood of a 3-connected planar graph is a triple (T_1, T_2, T_3) of oriented spanning trees such that every edge is contained in at least one and at most two trees and certain conditions on the edge order around each vertex hold (we give a precise definition in Section 2). For every pair (T_i, T_j) , $i \neq j$, the edges that are contained in both T_i and T_j induce paths. The third tree T_l , $l \notin \{i, j\}$ may then be used to arrange these paths in an order. This way we obtain a so-called *ordered path partition compatible* to the Schnyder wood (T_1, T_2, T_3) , which is nothing else than an ordered partition of the vertices of a graph into vertex sets of paths. By choosing (T_i, T_j) in all possible ways, every Schnyder wood generates three such compatible ordered path partitions; Fig. 1 provides an illustration. Ordered path partitions may also be seen as a generalization of canonical orderings [2,5,6]. We give a formal definition of Schnyder woods, ordered path partitions and how these two concepts relate in Section 2.

Our first result gives a new lower bound on the total number of leaves of the three trees of the unique minimal Schnyder wood (in the sense of the definition in Section 2), from which also a bound for one of these trees can be derived by pigeonhole principle (see Section 4). For the special case of triangulated planar graphs, a result of Bonichon et al. [3] shows

* Corresponding author.

E-mail address: christian.ortlieb@uni-rostock.de (C. Ortlieb).

¹ This research is supported by the grant SCHM 3186/2-1 (401348462) from the Deutsche Forschungsgemeinschaft (DFG, German Research Foundation).

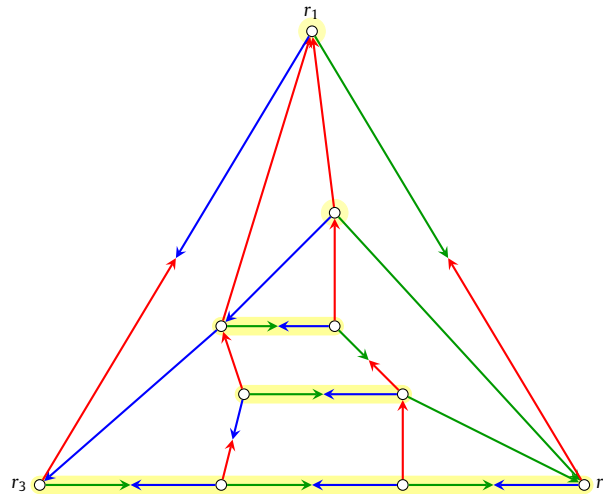


Fig. 1. A 3-connected planar graph and one of its Schnyder woods. The three trees of the Schnyder wood are depicted in colors red, blue and green, and are oriented towards the roots r_1 , r_2 and r_3 , respectively. One of the three compatible ordered path partitions, namely the one partitioning into green-blue paths, is marked in fat yellow; this ordered path partition contains exactly two singletons. (For interpretation of the colors in the figure(s), the reader is referred to the web version of this article.)

that there is such a tree with at least $n - \lfloor \frac{n-1+\Delta}{3} \rfloor$ leaves for any Schnyder wood, where Δ is the number of three colored faces in the Schnyder wood and n is the number of vertices. He and Zhang [19] also considered triangulated planar graphs and proved that there is such a tree with at least $(n + 1)/2$ leaves for the minimal Schnyder wood. They used this to show that every plane graph has a visibility representation by non-overlapping horizontal segments of height at most $\lceil 15n/16 \rceil$. They also gave the so far best bound of $2n/3 + O(1)$ for the height of such a visibility representation [20]. An upper bound of $2n + 1$ on the total number of leaves of any Schnyder wood of a 3-connected planar graph has been given by Kindermann et al. [16].

We consider the general case of 3-connected planar graphs and show that the minimal Schnyder wood has a tree with at least $n/5$ leaves; this bound is tight. As corollaries, we obtain slightly better results for triangulated planar graphs than the known ones before.

Our second result uses similar proof techniques and concerns *singletons*, that is, paths that consist of exactly one vertex, in compatible ordered path partitions of Schnyder woods. To the best of our knowledge, we are the first to investigate this parameter. Let G be a 3-connected plane graph of order n and let $f_{\neq 6}$ be the number of faces of G that are not of size 6. We show that at least one of the three compatible ordered path partitions contains $f_{\neq 6}/6$ singletons. We also show that for the minimal Schnyder wood of G at least one of the three compatible ordered path partitions contains $n/5$ singletons. Both bounds are tight and are given in Section 3. However, if we allow to choose a Schnyder wood of the given graph, we can give a bound that is slightly better. We show that there is a Schnyder wood of G (possibly different from the minimal one) that has a compatible ordered path partition with strictly more than $n/5$ singletons.

2. Schnyder woods and ordered path partitions

We define Schnyder woods and ordered path partitions, show how these two relate and give some basic properties that we need for the proofs. We only consider simple undirected graphs. A graph is *plane* if it is planar and embedded into the Euclidean plane.

2.1. Schnyder woods

Let r_1 , r_2 and r_3 be three vertices of the outer face boundary of a plane graph G in clockwise order. The $\{r_1, r_2, r_3\}$ -suspension G^σ of G is the graph obtained from G by adding at each vertex of $\{r_1, r_2, r_3\}$ a half-edge, an arc pointing into the outer face. We call r_1 , r_2 and r_3 *roots* and will often omit the quantifier $\{r_1, r_2, r_3\}$ if it is clear from the context.

Definition 1. Let G^σ be the $\{r_1, r_2, r_3\}$ -suspension of a 3-connected plane graph. A *Schnyder wood* of G^σ is an orientation and coloring of the edges of G^σ (including the half-edges) with the colors **1, 2, 3** (red, green, blue) such that

- (a) Every edge e is oriented in one direction (we say e is *unidirected*) or in two opposite directions (we say e is *bidirected*). Every direction of an edge is colored with one of the three colors **1, 2, 3** (we say an edge is *i-colored* if one of its directions has color i) such that the two colors i and j of every bidirected edge are distinct (we call such an edge *i-j-colored*). Throughout the paper, we assume modular arithmetic on the colors **1, 2, 3** such that $i + 1$ and $i - 1$ for a

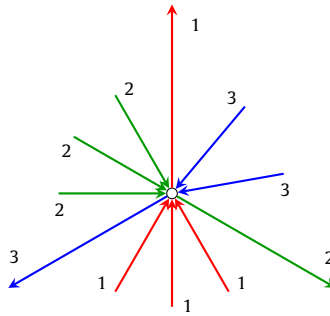


Fig. 2. Properties of Schnyder woods. Condition 1(c) at a vertex. Color 1 is depicted in red, color 2 in green and color 3 in blue as for the rest of the paper.

color i are defined as $(i \bmod 3) + 1$ and $(i + 1 \bmod 3) + 1$ respectively. For a vertex v , an incident uni- or bidirected edge is *ingoing* (i -colored) in v if it has a direction (of color i) that is directed toward v , and *outgoing* (i -colored) of v if it has a direction (of color i) that is directed away from v .

- (b) For every color i , the half-edge at r_i is undirected, outgoing and i -colored.
- (c) Every vertex v has exactly one outgoing edge of every color. The outgoing 1-, 2-, 3-colored edges e_1, e_2, e_3 of v occur in this clockwise order around v . For every color i , every ingoing i -colored edge of v is contained in the clockwise sector around v from e_{i+1} to e_{i-1} (see Fig. 2).
- (d) No inner face boundary contains a directed cycle (disregarding possible opposite directions) in one color.

For ease of notation, let $N^l(v)$ for a vertex v be the neighbors of v that share a bidirected edge with v . Also, if the choice of the roots is clear from context, we might speak of Schnyder woods of a graph G instead of Schnyder woods of the suspension of G .

Lemma 2 (e.g. Felsner [10]). *Every 3-connected plane graph admits a Schnyder wood.*

For a Schnyder wood and color i , let T_i be the directed graph that is induced by the directed edges of color i . The following result justifies the name of Schnyder woods.

Lemma 3 (Schnyder [18], Felsner [11]). *For every color i of a Schnyder wood of a graph G , T_i is a directed spanning tree of G in which all edges are oriented towards the root r_i .*

Although, the following lemma is widely known, we give a short proof for the sake of self-containedness of the paper.

Lemma 4. *Consider a Schnyder wood of a 3-connected planar graph G . Then G is internally triangulated (i.e. every face except the outer face is a triangle) if and only if every internal edge of G (i.e. an edge that is not incident to the outer face) is undirected in the Schnyder wood.*

Proof. Assume that G is internally triangulated. Every edge on the boundary of the outer face of G is bidirected [11, Theorem 2.3]. Let n, e and f be the number of vertices, edges and faces of G , respectively. Let C be the boundary of the outer face. Observe that G is internally triangulated if and only if every internal edge is on the boundary of two faces and every internal face is a triangle. We obtain that every internal edge is on the boundary of two faces and every internal face is a triangle if and only if $3(f - 1) = 2(e - |C|) + |C|$. Together with Euler's formula we obtain

$$\begin{aligned}
 3(f - 1) &= 2(e - |C|) + |C| \\
 \Leftrightarrow 3f &= 2e - |C| + 3 \\
 \Leftrightarrow 3n - 3e + 2e - |C| + 3 &= 6 \\
 \Leftrightarrow 3n - 3 &= e + |C|.
 \end{aligned}$$

Remember that at every vertex which is not a root vertex there are exactly three outgoing edges by Definition 1(c). The three root vertices have two outgoing edges and one outgoing half-edge each. So the left hand side of the above formula is the sum of the out-degrees. Since the edges on C are bidirected, this formula holds if and only if every internal edge is undirected. \square

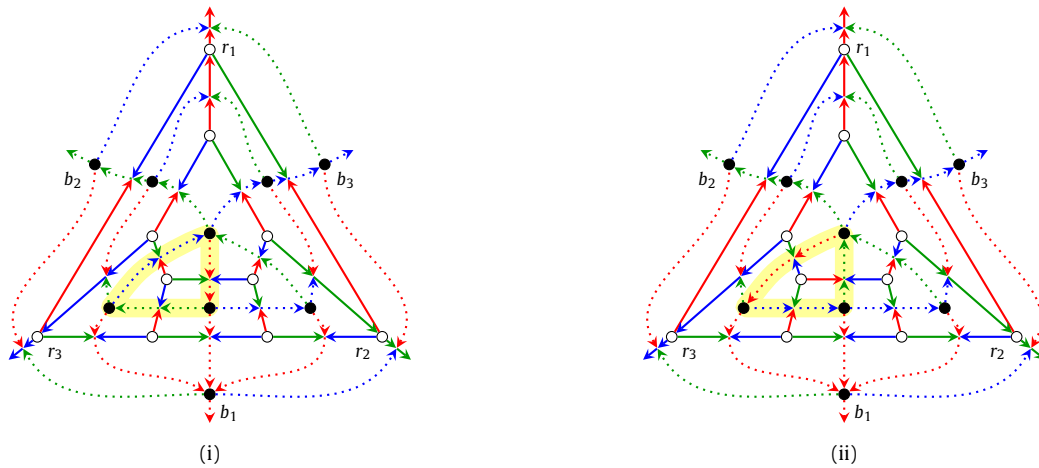


Fig. 3. The completion of G obtained by superimposing G^σ and its suspended dual G^{σ^*} (the latter depicted with dotted edges). The primal Schnyder wood in Fig. 3i is not the minimal element of the lattice of Schnyder woods of G , as this completion contains a clockwise directed cycle (marked in yellow). In Fig. 3ii this clockwise cycle has been flipped.

2.2. Dual Schnyder woods

Let G be a 3-connected plane graph. Any Schnyder wood of G^σ with roots r_1, r_2 and r_3 induces a Schnyder wood of a slightly modified planar dual of G^σ in the following way [8,12] (see [15, p. 30] for an earlier variant of this result given without proof). As common for plane duality, we will use the plane dual operator $*$ to switch between primal and dual objects (also on sets of objects).

Extend the three half-edges of G^σ to non-crossing infinite rays and consider the planar dual of this plane graph. Since the infinite rays partition the outer face f of G into three parts, this dual contains a triangle with vertices b_1, b_2 and b_3 instead of the outer face vertex f^* such that b_i^* is not incident to r_i for every i (see Fig. 3). Let the *suspended dual* G^{σ^*} of G be the graph obtained from this dual by adding at each vertex of $\{b_1, b_2, b_3\}$ a half-edge pointing into the outer face.

Consider the superposition of G^σ and its suspended dual G^{σ^*} such that exactly the primal dual pairs of edges cross (here, for every $1 \leq i \leq 3$, the half-edge at r_i crosses the dual edge $b_{i-1}b_{i+1}$).

Definition 5. For any Schnyder wood S of G^σ , define the orientation and coloring S^* of the suspended dual G^{σ^*} as follows (see Fig. 3):

- (a) For every unidirected $(i - 1)$ -colored edge or half-edge e of G^σ , color e^* with the two colors i and $i + 1$ such that e points to the right of the i -colored direction.
- (b) Vice versa, for every $i - (i + 1)$ -colored edge e of G^σ , $(i - 1)$ -color e^* unidirected such that e^* points to the right of the i -colored direction.
- (c) For every color i , make the half-edge at b_i unidirected, outgoing and i -colored.

The following lemma states that S^* is indeed a Schnyder wood of the suspended dual. By Definition 5(c), the vertices b_1, b_2 and b_3 are the roots of S^* .

Lemma 6 ([14][12, Prop. 3]). For every Schnyder wood S of G^σ , S^* is a Schnyder wood of G^{σ^*} .

Lemma 6 gives a bijection between the Schnyder woods of G^σ and the ones of G^{σ^*} . Let the *completion* \tilde{G} of G be the plane graph obtained from the superposition of G^σ and G^{σ^*} by subdividing each pair of crossing (half-)edges with a new vertex, which we call a *crossing vertex* (see Fig. 3). The completion has six half-edges pointing into its outer face.

Any Schnyder wood S of G^σ implies the following natural orientation and coloring \tilde{G}_S of its completion \tilde{G} . For every edge $vw \in E(G^\sigma) \cup E(G^{\sigma^*})$, we do the following. Let z be the crossing vertex of G^σ that subdivides vw and consider the coloring of vw in either S or S^* . If vw is outgoing of v and i -colored, we direct $vz \in E(\tilde{G})$ toward z and i -color it. We do the same for w . In the remaining case that vw is unidirected, ingoing in v and i -colored, we direct $zv \in E(\tilde{G})$ toward v and i -color it. The three half-edges of G^{σ^*} inherit the orientation and coloring of S^* for \tilde{G}_S . By Definition 5, the construction of \tilde{G}_S implies immediately the following corollary.

Corollary 7. Every crossing vertex of \tilde{G}_S has one outgoing edge and three ingoing edges and the latter are colored 1, 2 and 3 in counterclockwise direction.

Using results on orientations with prescribed outdegrees on the respective completions, Felsner and Mendez [7,11] showed that the set of Schnyder woods of a planar suspension G^σ forms a distributive lattice. The order relation of this lattice relates a Schnyder wood of G^σ to a second Schnyder wood if the former can be obtained from the latter by reversing the orientation of a directed clockwise cycle in the completion. We refer to such an operation as a *flip* of that cycle. Such a flip also includes the necessary changes of the colors of the edges on the cycle and in its interior. If we flip, for example, a clockwise cycle, then an i -colored edge on the cycle is $(i + 1)$ -colored after the flip and an i -colored edge in the interior of the cycle becomes $(i - 1)$ -colored (Fig. 3). This gives the following lemma, of which the computational part is due to Fusy [13].

Lemma 8 ([7,11,13]). *For the minimal element S of the lattice of all Schnyder woods of G^σ , \tilde{G}_S contains no clockwise directed cycle. Also, S and \tilde{G}_S can be computed in linear time.*

We call the minimal element of the lattice of all Schnyder woods of G^σ also the *minimal Schnyder wood* of G^σ . Verifying that a given Schnyder wood S of a graph G is indeed minimal can be cumbersome. We give the following tool to facilitate this. Let v_1, \dots, v_l be an order of the vertices of \tilde{G}_S such that for every $k \in \{1, \dots, l\}$ and $A_k := \{v_1, \dots, v_k\}$ the vertex v_k is not in a clockwise cycle of $\tilde{G}_S[A_k]$. Call an order like that an *elimination order* for \tilde{G}_S . Now, the following two lemmas allow to easily verify that a given Schnyder wood is minimal.

Lemma 9. *Let G be a 3-connected plane graph and S a Schnyder wood of G . S is minimal if and only if there exists an elimination order of \tilde{G}_S .*

Proof. If S is minimal, then any order of the vertices is an elimination order.

So assume we have an elimination order v_1, \dots, v_l of \tilde{G}_S . Let $A_k = \{v_1, \dots, v_k\}$. We show by induction that $\tilde{G}_S[A_k]$ does not have a clockwise cycle for $k = 1, \dots, l$. $\tilde{G}_S[A_1]$ is a single vertex and thus it does not have a clockwise cycle. Let $2 \leq k \leq l$. For the sake of contradiction, assume that there is a clockwise cycle C in $\tilde{G}_S[A_k]$. The vertex v_k is not in a clockwise cycle of $\tilde{G}_S[A_k]$. So C does not contain v_k . And hence C has only vertices in $\{v_1, \dots, v_{k-1}\}$. We obtain that C is also in $\tilde{G}_S[A_{k-1}]$, contradicting the induction hypothesis. So $\tilde{G}_S[A_k]$ does not contain a clockwise cycle. \square

Lemma 10. *Every order v_1, \dots, v_l of the vertices of \tilde{G}_S that satisfies one of the following properties for every $k \in \{1, \dots, l\}$ is an elimination order of S .*

- (a) v_k has no ingoing or no outgoing edges in $\tilde{G}_S[A_k]$.
- (b) v_k has exactly one outgoing edge e and e appears in counterclockwise direction on the outer face boundary of $\tilde{G}_S[A_k]$.
- (c) $v_k \in \{r_1, r_2, r_3, b_1, b_2, b_3\}$.

Proof. We need to show that a vertex v_k with one of the above properties cannot be on a clockwise cycle in $\tilde{G}_S[A_k]$. If v_k has property (a), then it cannot be on an oriented cycle of $\tilde{G}_S[A_k]$ and hence not on a clockwise cycle of $\tilde{G}_S[A_k]$.

Now, we consider property (c). Assume that w.l.o.g. $v_k = b_1$. The outgoing half-edge at b_1 cannot be on a clockwise cycle. The vertex b_1 has two more outgoing edges e and e' in \tilde{G}_S ending on the crossing vertices x and x' which subdivide the half-edges in G^σ of r_2 and r_3 , respectively. See Fig. 3 for illustration. So if there is an oriented cycle C containing b_1 , then it contains w.l.o.g. x . But x has only one outgoing (half-)edge in \tilde{G}_S , namely, the half-edge originating from the half-edge of r_2 in G^σ . This half-edge cannot be on an oriented cycle and thus x cannot be on an oriented cycle. Similar arguments yield that all oriented paths starting at w.l.o.g. r_2 with an outgoing edge either pass through b_3, b_1 or the crossing vertex x . As observed above, those vertices cannot be on an oriented cycle. And thus r_2 cannot be on an oriented cycle.

It remains to show that if v_k has property (b), it cannot be on a clockwise cycle in $\tilde{G}_S[A_k]$. Let e be the outgoing edge at v_k . If v_k is on a clockwise cycle C , then e needs to be an edge of C since it is the only outgoing edge at v_k . But since e appears in counterclockwise direction on the outer face of $\tilde{G}_S[A_k]$ it cannot be on a clockwise cycle in $\tilde{G}_S[A_k]$, a contradiction. \square

2.3. Ordered path partitions

Definition 11 ([2,17]). Let G be a plane 3-connected graph with three vertices r_1, r_2 and r_3 in that clockwise order on the outer face. An *ordered path partition* $\mathcal{P} = (P_0, \dots, P_s)$ of G with *base-pair* (r_j, r_{j+1}) is an ordered partition of $V(G)$ into the vertex sets of induced paths such that the following holds for every $i \in \{0, \dots, s - 1\}$, where $V_i := \bigcup_{q=0}^i P_q$ and the *contour* C_i is the clockwise walk from r_{j+1} to r_j on the outer face of $G[V_i]$.

- (a) P_0 is the vertex set of the clockwise path from r_j to r_{j+1} on the outer face boundary of G , and $P_s = \{r_{j+2}\}$.
- (b) Every vertex in P_i has at least one neighbor in $V(G) \setminus V_i$.
- (c) C_i is a path.
- (d) Every vertex in C_i has at most one neighbor in P_{i+1} .

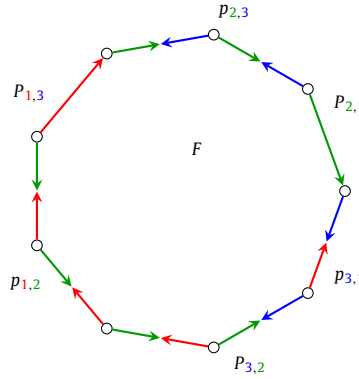


Fig. 4. Illustration for Lemma 12. An internal face \$F\$ and the paths on its boundary. Here, \$P_{1,3}\$ has only color 1, \$P_{2,1}\$ has only color 2 and \$P_{3,2}\$ is 2-3-colored.

For the ease of notation we often refer to vertex sets of paths as paths.
 As proven in [2, Theorem 5] and [1, Lemma 1], the vertex sets of the inclusion-wise maximal \$j\$-\$(j + 1)\$-colored paths of any Schnyder wood \$S\$ of a suspension \$G^\sigma\$, \$j \in \{1, 2, 3\}\$ form an ordered path partition of \$G\$ with base pair \$(r_j, r_{j+1})\$; we call this special ordered path partition *compatible* with \$S\$ and denote it by \$\mathcal{P}^{j,j+1}\$ (Fig. 1).
 By Definition 11(a) and 11(b), \$G\$ contains for every \$i\$ and every vertex \$v \in P_i\$ a path from \$v\$ to \$r_{j+2}\$ that intersects \$V_i\$ only in \$v\$. Since \$G\$ is plane, this implies that every path \$P_i\$ is embedded into the outer face of \$G[V_{i-1}]\$ for every \$1 \le i \le s\$.
 As shown in [1,2,17] compatible ordered path partitions have a specific structure. Consider for example \$\mathcal{P}^{2,3} = (P_0, \dots, P_s)\$. Every path of this ordered path partition is, as stated above, a maximal 2-3-colored path. Let \$P_i = \{v_1, \dots, v_k\}\$, \$i \in \{1, \dots, s\}\$ be such that \$v_1\$ is the first vertex of \$P_i\$ in clockwise direction on the outer face of \$G[V_i]\$ and \$v_k\$ is the last. Then there is an edge \$v_1x\$ on the outer face of \$G[V_i]\$ that connects \$v_1\$ to a vertex \$x\$ of \$V_{i-1}\$. This edge is outgoing 3-colored at \$v_1\$. Similarly, we find an edge \$v_kx'\$ at \$v_k\$ such that \$x' \in V_{i-1}\$ and \$v_kx'\$ is on the outer face of \$G[V_i]\$. This edge is outgoing 2-colored at \$v_k\$. Every other edge that connects a vertex of \$P_i\$ with a vertex of \$V_{i-1}\$ is unidirected 1-colored and ingoing at a vertex of \$P_i\$.
 A path which has only one vertex is called a *singleton*. For a vertex \$v \in V(G)\$ define the *multiplicity* \$m(v) := |\{i \in \{1, 2, 3\} \mid v \text{ is a singleton in } \mathcal{P}^{i,i+1}\}|\$.
 For a face \$F\$ of a planar graph define the size \$|F|\$ to be the number of vertices it is incident to.

3. Singletons

Remember that, given a Schnyder wood of a 3-connected planar graph, the maximal \$i\$-\$(i + 1)\$-colored paths form the compatible ordered path partition \$\mathcal{P}^{i,i+1}\$. In a compatible ordered path partition, a singleton is a path that consists of exactly one vertex. Here, we give two tight lower bounds on the number of singletons in compatible ordered path partitions. One lower bound is in terms of \$f_{\neq 6}\$, the number of faces that do not have size 6, and the other is in terms of the number of vertices.

Lemma 12 (Di Battista, Tamassia, Vismara [8]). *Let \$G\$ be a 3-connected planar graph and let a Schnyder wood on \$G\$ be given. An internal face of \$G\$ consists of six clockwise consecutive paths \$P_{3,2}, p_{1,2}, P_{1,3}, p_{2,3}, P_{2,1}\$ and \$p_{3,1}\$ (Fig. 4) where:*

- for every \$i, j \in \{1, 2, 3\}\$, with \$i \neq j\$, \$P_{i,j}\$ consists of one edge that is either clockwise colored \$i\$, counterclockwise colored \$j\$ or both,
- for every \$i, j \in \{1, 2, 3\}\$, with \$i \neq j\$, \$p_{i,j}\$ consists of a possibly empty sequence of edges all colored clockwise \$i\$ and counterclockwise \$j\$.

The external face of \$G\$ consists of 3 clockwise consecutive paths \$p_{2,1}, p_{3,2}\$ and \$p_{1,3}\$.

Theorem 13. *Let \$S\$ be a Schnyder wood of a 3-connected plane graph \$G\$. Then one of the three ordered path partitions that are compatible with \$S\$ has at least \$\lceil \frac{f_{\neq 6}}{6} \rceil\$ singletons, where \$f_{\neq 6}\$ is the number of faces of \$G\$ that are not of size six.*

Proof. Let \$r_1, r_2\$ and \$r_3\$ be the roots of \$S\$. Define

$$E_{uni} := \{e \in E(G) \mid e \text{ is unidirected}\}$$

$$V_{bi} := \{v \in V(G) \mid v \text{ is incident to two edges that both have the same two colors}\}.$$

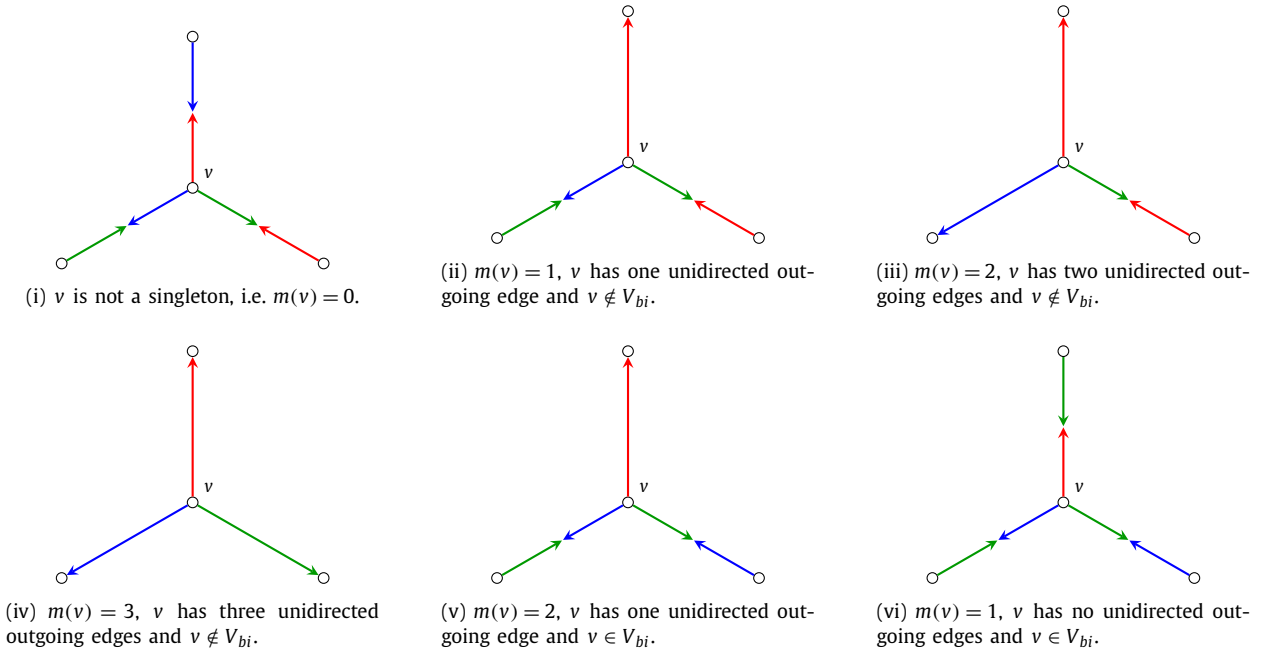


Fig. 5. The six possible cases for the outgoing edges of a vertex $v \in V(G) \setminus \{r_1, r_2, r_3\}$ (up to symmetry).

Now, we show how E_{uni} and V_{bi} relate to the number of singletons. Consider the outgoing edges of a vertex $v \in V(G) \setminus \{r_1, r_2, r_3\}$. Observe that, up to symmetry, there are six possible colorings for those edges. They are depicted in Fig. 5. In Fig. 5ii, the three outgoing edges of v are all bidirected such that no two have the same two colors. In Fig. 5iii, exactly two of the three outgoing edges at v is unidirected and the remaining two do not have the same two colors. In Fig. 5iii, exactly two of the three outgoing edges are unidirected. In Fig. 5iv, the three outgoing edges of v are all unidirected. In Fig. 5v, one outgoing edge of v is unidirected and the other two have the same two colors. In Fig. 5vi, all the outgoing edges of v are bidirected and two of those have the same colors. By Definition 1(c), the three outgoing edges at v cannot all have the same two colors. So this case distinction is exhaustive.

We observe that a vertex $v \in V(G) \setminus \{r_1, r_2, r_3\}$ is a singleton in exactly one compatible ordered path partition if and only if either v has exactly one unidirected outgoing edge and $v \notin V_{bi}$ or $v \in V_{bi}$, see Fig. 5vi and 5ii. Similarly, v is a singleton in exactly two compatible ordered path partitions if and only if it either has exactly two outgoing unidirected edges or $v \in V_{bi}$ and it has exactly one outgoing unidirected edge, see Fig. 5iii and 5v. And v is a singleton in exactly three compatible ordered path partitions if and only if v has exactly three outgoing unidirected edges, see Fig. 5iv. Additionally, we know that each of the roots r_1, r_2 and r_3 is a singleton in exactly one compatible ordered path partition. We therefore obtain the following equation.

$$\sum_{i=1}^3 |\{v \mid v \text{ is a singleton in } \mathcal{P}^{i,i+1}\}| = 3 + |E_{uni}| + |V_{bi}|.$$

In the following, let $n := |V(G)|$, $m := |E(G)|$, f be the number of faces of G and $f_{<6}$, $f_{>6}$ and $f_{\geq 6}$ be the number of faces of G of size smaller than 6, larger than 6 and at least 6, respectively. Every vertex $v \in V(G) \setminus \{r_1, r_2, r_3\}$ has $\deg(v) - 3$ ingoing unidirected edges. A root vertex $v \in \{r_1, r_2, r_3\}$ has $\deg(v) - 2$ such edges. Together with the handshake lemma this yields that

$$\begin{aligned} |E_{uni}| &= \sum_{v \in V(G) \setminus \{r_1, r_2, r_3\}} (\deg(v) - 3) + \sum_{i=1}^3 (\deg(r_i) - 2) \\ &= 3 + \sum_{v \in V(G)} (\deg(v) - 3) = 3 - 3n + 2m. \end{aligned}$$

Now, we give a bound on $|V_{bi}|$. Consider a face F of G . Let v be a vertex of $p_{i,i+1}$ such that v is incident to two $i-(i+1)$ -colored edges, for some i in $\{1, 2, 3\}$. Here $p_{i,i+1}$ is defined as in Lemma 12. Observe that $v \in V_{bi}$. Also, by Lemma 12, for every face F of G with $|F| \geq 6$ there are at least $|F| - 6$ such vertices. And thus we obtain that

$$|V_{bi}| \geq \sum_{\substack{F \text{ face of } G, \\ |F| \geq 6}} (|F| - 6).$$

Together with Euler's polyhedral formula ($n - m + f = 2$) and $2m = \sum_{F \text{ face of } G} |F|$ this gives

$$\begin{aligned} \sum_{i=1}^3 |\{v \mid v \text{ is a singleton in } \mathcal{P}^{i,i+1}\}| &= 3 + |E_{uni}| + |V_{bi}| \\ &\geq 3 + 3 - 3n + 2m + \sum_{\substack{F \text{ face of } G, \\ |F| \geq 6}} (|F| - 6) \\ &= 6 - 3(2 - f + m) + 2m + \sum_{\substack{F \text{ face of } G, \\ |F| \geq 6}} (|F| - 6) \\ &= 3f - m - 6f_{\geq 6} + \sum_{\substack{F \text{ face of } G, \\ |F| \geq 6}} |F| \\ &= 3f - \frac{1}{2} \sum_{F \text{ face of } G} |F| - 6f_{\geq 6} + \sum_{\substack{F \text{ face of } G, \\ |F| \geq 6}} |F| \\ &= 3f_{<6} - \frac{1}{2} \sum_{\substack{F \text{ face of } G, \\ |F| < 6}} |F| - 3f_{\geq 6} + \frac{1}{2} \sum_{\substack{F \text{ face of } G, \\ |F| \geq 6}} |F| \\ &\geq 3f_{<6} - \frac{5}{2}f_{<6} - 3f_{>6} + \frac{7}{2}f_{>6} \\ &= \frac{1}{2}f_{<6} + \frac{1}{2}f_{>6} \\ &= \frac{f_{\neq 6}}{2}. \end{aligned}$$

By pigeonhole principle, there exists an ordered path partition that has at least $\lceil \frac{f_{\neq 6}}{6} \rceil$ singletons. \square

Remark. The bound of Theorem 13 is tight: there is a sequence of graphs G_k together with a Schnyder wood S_k such that

$$\frac{\sum_{i=1}^3 |\{v \mid v \text{ is a singleton in } \mathcal{P}^{i,i+1} \text{ of } G_k\}|}{|\{f \mid f \text{ is a face of } G_k \text{ and } |f| \neq 6\}|} \rightarrow \frac{1}{2}, \text{ for } k \rightarrow \infty.$$

The graphs G_k , which we define in the following, are symmetric with respect to $\mathcal{P}^{1,2}$, $\mathcal{P}^{2,3}$ and $\mathcal{P}^{3,1}$. Hence, every compatible ordered path partition has the same number of singletons. In the end, we obtain that for every $\varepsilon > 0$ there exists a graph G_k such that all three ordered path partitions have at most $\lfloor (\frac{1}{6} + \varepsilon) \cdot |\{f \mid f \text{ is a face of } G_k \text{ and } |f| \neq 6\}| \rfloor$ singletons each.

We show how to obtain the graphs G_k . First, we define a substructure which we call flower. Using those flowers, we iteratively bind a triangular bouquet of flowers of side length k , called B_k . In order to obtain the graph G_k , we only need to add three root vertices and their incident edges to B_k . Then we explicitly compute the number of singletons and the number of faces and show that our claim holds.

We start with flowers. Let a flower F be a plane graph with oriented and colored edges defined as follows. Let $V(F) = \{c_0, \dots, c_{17}, c\}$. The vertices c_0, \dots, c_{17} form a cycle in clockwise direction. We add the vertex c in the middle of the cycle and add the edges $c_i c$ for $i \in \{0, 3, 6, \dots, 15\}$. The edges are colored as in Fig. 6.

In order to bind the triangular bouquet of flowers, we need to define how flowers are combined. So let F and F' be two flowers with $V(F) = \{c_0, \dots, c_{17}, c\}$ and $V(F') = \{c'_0, \dots, c'_{17}, c'\}$. In the following, we define three different gluing operations. We say that we glue F' to the east of F if we identify the vertex pairs $(c_{10}, c'_4), (c_{11}, c'_3), (c_{12}, c'_2), (c_{13}, c'_1)$ and the edges in between those. Their colors match (see Fig. 7). Gluing F' to the southwest of F identifies the vertex pairs $(c_1, c'_7), (c_0, c'_8), (c_{17}, c'_9), (c_{16}, c'_{10})$ and the edges in between those pairs. The third gluing operation is gluing F' to the southeast of F . Here, we identify the vertex pairs $(c_{16}, c'_4), (c_{15}, c'_5), (c_{14}, c'_6), (c_{13}, c'_7)$ and the edges in between. It is easy to confirm that the colors of the identified edges match (see Fig. 8).

Now, we iteratively define a triangular bouquet of flowers B_k of side length k . Starting with B_1 , which is a single flower, we call this flower F_1^1 . In order to obtain B_k , take B_{k-1} and add k flowers F_k^1, \dots, F_k^k as follows. Glue F_k^1 to the east of F_{k-1}^1 .

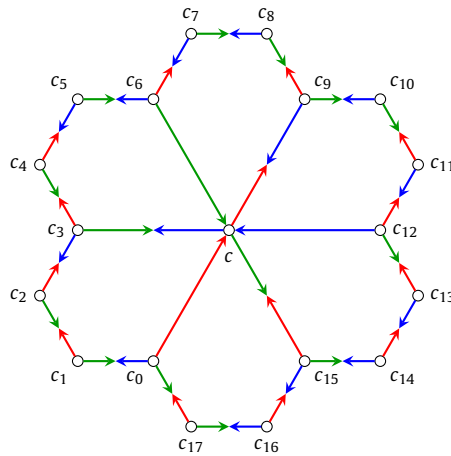


Fig. 6. A flower and its edge colors.

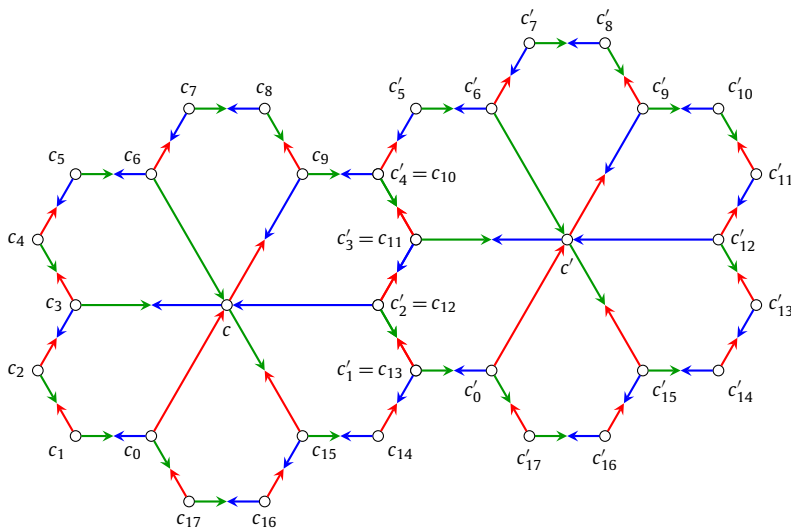


Fig. 7. Gluing the flower F' to the east of F .

For all $i \in \{2, \dots, k - 1\}$, glue F_k^i to the east of F_{k-1}^i , to the southeast of F_{k-1}^{i-1} and to the southwest of F_k^{i-1} . In the end, glue F_k^k to the southeast of F_{k-1}^{i-1} and to the southwest of F_k^{i-1} . See Fig. 8 for an example.

The graph G_k is constructed by taking B_k and adding three vertices r_1, r_2 and r_3 in the outer face. We add the edges r_1r_2 (1-2-colored), r_2r_3 (2-3-colored) and r_3r_1 (1-3-colored). Now, every vertex that does not have an outgoing i -colored edge becomes connected to r_i with an outgoing i -colored edge for all $i \in \{1, 2, 3\}$. We also add the half-edges at the vertices r_1, r_3 and r_2 and color them accordingly. See Fig. 9 for an example.

It is easy to confirm that the orientation and coloring of G_k is indeed a Schnyder wood. Definition 1(a) and (b) are met by construction. In Fig. 9, we observe that Definition 1(c) holds for every vertex. For Definition 1(d) we need to confirm that no face has a boundary which is a directed cycle in one color. In Fig. 6, we observe that this holds for all the internal faces of flowers. In Fig. 9, we see that this also holds for the remaining faces. So we have a Schnyder wood.

Now, we count the singletons and the faces of G_k . Let $v \in V(G_k) \setminus \{r_1, r_2, r_3\}$. Observe, in Fig. 9, that either v has one unidirected outgoing edge and two bidirected outgoing edges that are colored differently or v has three bidirected outgoing edges such that no two share the same two colors. So, up to symmetry, the situation at v is either as in Fig. 5i or as in Fig. 5ii. Thus, every unidirected edge gives rise to exactly one singleton. And, on the internal vertices, this assignment is bijective. Every flower has three unidirected edges. There are $\frac{k \cdot (k+1)}{2}$ flowers in G_k . Together with the edges incident to the root vertices, we have $3 \cdot (3k + 1) + 3 \cdot \frac{k \cdot (k+1)}{2}$ unidirected edges. Since the root vertices are also singletons in exactly one compatible ordered path partition, we obtain that $\sum_{i=1}^3 |\{v \mid v \text{ is a singleton in } \mathcal{P}^{i,i+1} \text{ of } G_k\}| = 3 + 3 \cdot (3k + 1) + 3 \cdot \frac{k \cdot (k+1)}{2}$.

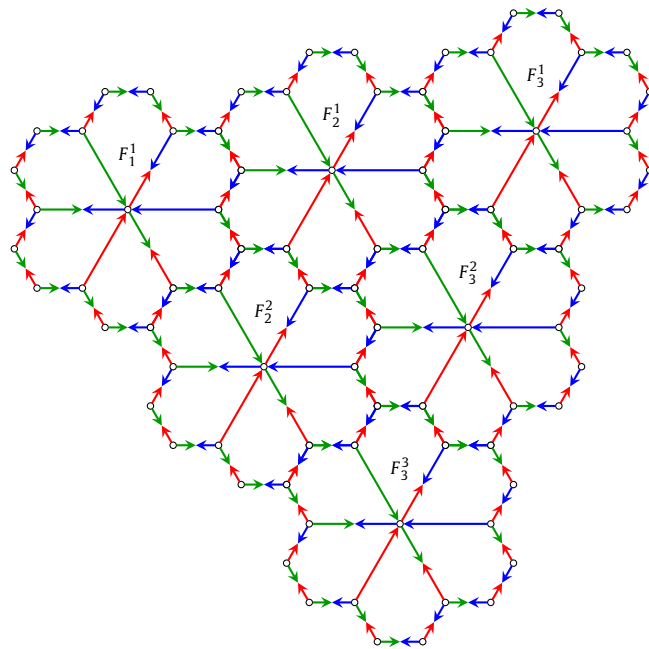


Fig. 8. The triangular bouquet of flowers B_3 .

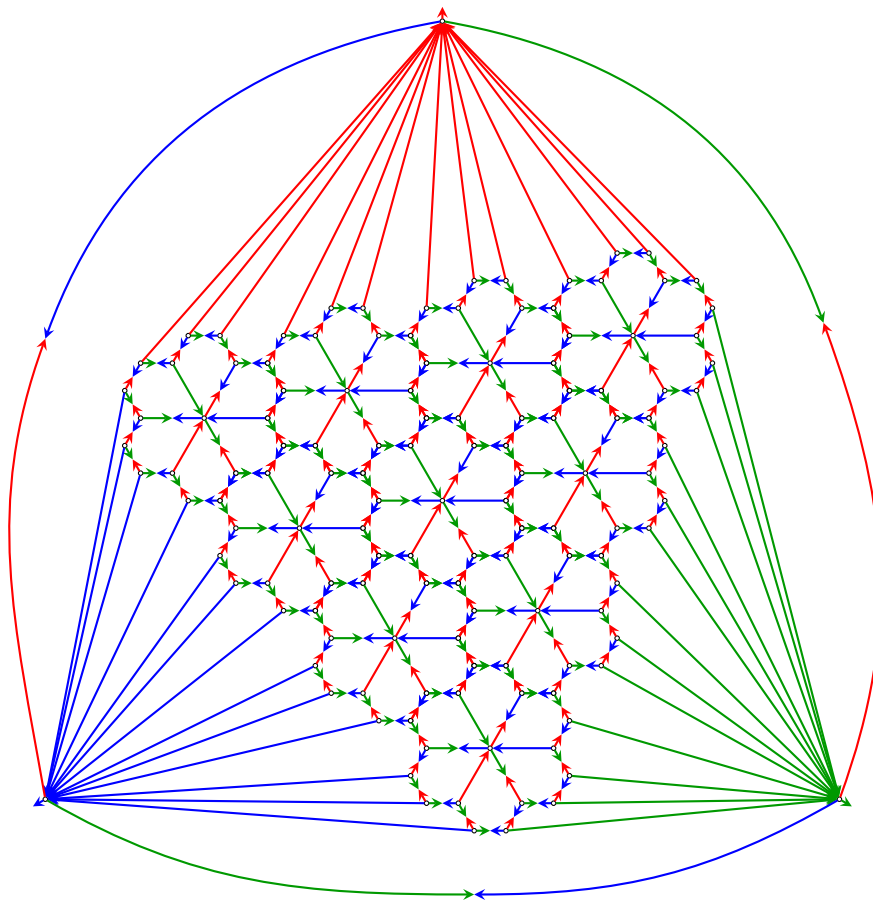


Fig. 9. The graph G_4 with its Schnyder wood.

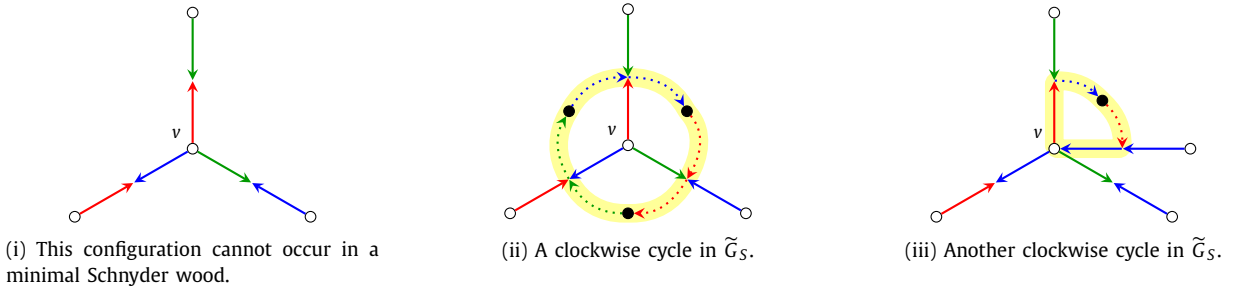


Fig. 10. The situation in the proof of Lemma 14.

Observe that there are no faces of size six. Every flower has six faces. Hence, the flowers give in total $6 \cdot \frac{k \cdot (k+1)}{2}$ faces. Counting also the faces incident to the root vertices and the outer face, we obtain that $|\{f \mid f \text{ is a face of } G_k \text{ and } |f| \neq 6\}| = 3 \cdot (3k + 1) + 1 + 6 \cdot \frac{k \cdot (k+1)}{2}$. And hence

$$\begin{aligned} & \frac{\sum_{i=1}^3 |\{v \mid v \text{ is a singleton in } \mathcal{P}^{i,i+1} \text{ of } G_k\}|}{|\{f \mid f \text{ is a face of } G_k \text{ and } |f| \neq 6\}|} \\ &= \frac{3 \cdot (3k + 1) + 3 + 3 \cdot \frac{k \cdot (k+1)}{2}}{3 \cdot (3k + 1) + 1 + 6 \cdot \frac{k \cdot (k+1)}{2}} \\ &= \frac{\frac{3}{2}k^2 + \frac{21}{2}k + 6}{3k^2 + 12k + 4} \longrightarrow \frac{1}{2}, \text{ for } k \rightarrow \infty. \end{aligned}$$

Observe that G_k is symmetric with respect to $\mathcal{P}^{1,2}$, $\mathcal{P}^{2,3}$ and $\mathcal{P}^{3,1}$. So every ordered path partition of G_k that is compatible with S_k has the same number of singletons. Hence, for every $\varepsilon > 0$ there exists a graph G_k such that all three ordered path partitions have at most $\lfloor (\frac{1}{6} + \varepsilon) \cdot |\{f \mid f \text{ is a face of } G_k \text{ and } |f| \neq 6\}| \rfloor$ singletons.

Lemma 14. Let G be a 3-connected planar graph and S be its minimal Schnyder wood. Then no vertex is incident to an edge colored outgoing 1 and ingoing 2, an edge colored outgoing 2 and ingoing 3 and an edge colored outgoing 3 and ingoing 1, see Fig. 10i for illustration.

Proof. Assume for the sake of contradiction that there exists such a vertex $v \in V(G)$. If v has degree three, then, by Corollary 7, there exists a clockwise cycle in \tilde{G}_S going through the three crossing vertices of the edges incident to v , see Fig. 10ii. If v has an ingoing edge in w.l.o.g. color 3, then, by Corollary 7, we can find a clockwise cycle in \tilde{G}_S containing v , see Fig. 10iii. In both cases, we arrive at a contradiction since the minimal Schnyder wood does not have clockwise cycles by Lemma 8. \square

Theorem 15. Let G be a 3-connected planar graph of order n and let S be a minimal Schnyder wood of G . Then

$$\sum_{i=1}^3 |\{v \mid v \text{ is a singleton in } \mathcal{P}^{i,i+1}\}| \geq \frac{3n}{5}.$$

Proof. Let $r_1, r_2, r_3 \in V(G)$ be the roots of S . Remember that S has exactly three compatible ordered path partitions. For $i = 1, 2, 3$, let

$$s_i := |\{v \mid v \text{ is a singleton in exactly } i \text{ of the compatible ordered path partitions of } S\}|.$$

Observe that $\sum_{i=1}^3 |\{v \mid v \text{ is a singleton in } \mathcal{P}^{i,i+1}\}| = \sum_{i=1}^3 i s_i \geq \sum_{i=1}^3 s_i$. In the following, we give a lower bound on $\sum_{i=1}^3 s_i$. The proof is by double counting vertices that are a singleton in one or two of the compatible ordered path partitions. Observe that a vertex that is not a singleton in $\mathcal{P}^{i,i+1}$ needs to be incident to at least one $i - (i + 1)$ -colored edge. So, by Lemma 14, a vertex which is no singleton in all three compatible ordered path partitions needs to be incident to an edge colored outgoing 1 and ingoing 3, an edge colored outgoing 2 and ingoing 1 and an edge colored outgoing 3 and ingoing 2, see Fig. 11. Call a vertex having this property a *Type-A vertex*. So there are exactly $(n - \sum_{i=1}^3 s_i)$ Type-A vertices.

Remember that by $N^l(v)$ we refer to the vertices that share a bidirected edge with v . If $v \in V(G)$ is a Type-A vertex, then, by the definition of Type-A vertices, the three vertices in $N^l(v)$ cannot be Type-A. So those three neighbors are singletons in either one or two of the three compatible ordered path partitions. By Lemma 14, a vertex v that is not Type-A has at most

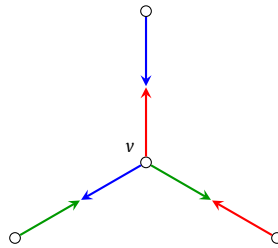


Fig. 11. A Type-A vertex v .

two neighbors in $N^l(v)$ that are Type-A. These two facts together imply the inequality marked by (\star) in the subsequent equation. Hence, we have

$$\sum_{i=1}^3 s_i \geq s_1 + s_2 \stackrel{(\star)}{\geq} \frac{3}{2} \cdot |\{v \in V(G) \mid v \text{ is Type-A}\}| = \frac{3}{2} (n - \sum_{i=1}^3 s_i)$$

$$\Rightarrow \sum_{i=1}^3 s_i \geq \frac{3n}{5}.$$

Since $\sum_{i=1}^3 |\{v \mid v \text{ is a singleton in } \mathcal{P}^{i,i+1}\}| \geq \sum_{i=1}^3 s_i$, the claim follows. \square

By pigeonhole principle, we obtain the following corollary.

Corollary 16. *Let G be a 3-connected planar graph of order n and let S be a minimal Schnyder wood of G . There exists a compatible ordered path partition $\mathcal{P}^{i,i+1}$ with $i \in \{1, 2, 3\}$ that has at least $\lceil n/5 \rceil$ singletons.*

Remark. The bound of Theorem 15 is tight. We show this in Theorem 26 of Section 4. The graph we need to show this also shows that our bound on the number of leaves is tight. So we present it later.

The following definition and lemmas are in preparation of Theorem 20. This theorem gives a bound on the number of singletons which is better than the bound of Theorem 15. But, we need to acquiesce that the respective Schnyder wood might not be the minimal Schnyder wood anymore. We do not expect the bound of Theorem 20 to be tight.

Remember that if we flip a counterclockwise cycle in \tilde{G}_S , then the orientation of all its edges is reversed and the edges on the cycle and in the interior of the cycle are recolored. An i -colored edge on the cycle is $(i - 1)$ -colored after the flip and an i -colored edge in the interior of the cycle becomes $(i + 1)$ -colored. Also, remember that by $m(v)$ we denote the multiplicity of a vertex v .

Definition 17. Let G be a 3-connected planar graph. For a Type-A vertex $v \in V(G)$, define the Type-A-neighborhood as $N^A(v) := \{x \mid x \neq v \text{ is Type-A and } N^l(x) \cap N^l(v) \neq \emptyset\}$ (Fig. 12).

Note that a vertex that is contained in the Type-A-neighborhood of v is not a neighbor of v , i.e., $N^A(v) \cap N(v) = \emptyset$.

Lemma 18. *Let G be a planar 3-connected graph with a minimal Schnyder wood. We obtain the following two statements.*

- (a) *For every $x \in V(G)$, the neighborhood $N^l(x)$ contains at most two Type-A vertices.*
- (b) *For every Type-A vertex v , we have that $|N^A(v)| \leq 3$ (Fig. 12).*
- (c) *And if $|N^A(v)| = 3$ for a Type-A vertex v , then for every $x \in N^l(v)$, the neighborhood $N^l(x)$ contains exactly two Type-A vertices.*

Proof. Consider the first statement. Assume for the sake of contradiction that there exists a vertex $x \in V(G)$ such that $N^l(x)$ contains at least three Type-A vertices. Remember that $N^l(x)$ consists of the vertices that are joined with x by a bidirected edge. Hence, $|N^l(x)| = 3$ by Definition 1(c). And, by Definition 1(c) and the definition of Type-A vertices, we obtain that the bidirected edges incident to x form exactly the configuration that is forbidden due to Lemma 14, a contradiction. This proves the first statement.

Now, we prove the second and third statement. Let v be a Type-A vertex. $N^l(v)$ contains three vertices and for those three vertices statement (a) applies. So every vertex x in $N^l(v)$, is adjacent to at most one Type-A vertex that is different from v . And thus, we obtain that $|N^A(v)| \leq 3$ by Definition 17. This proves the second statement. We also observe that if $|N^A(v)| = 3$, then every vertex x in $N^l(v)$, needs to be adjacent to exactly one Type-A vertex that is different from v . This shows the third statement. \square

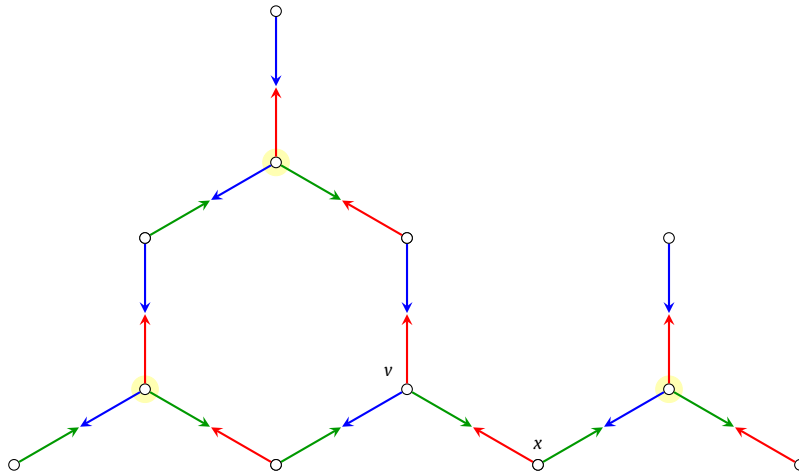
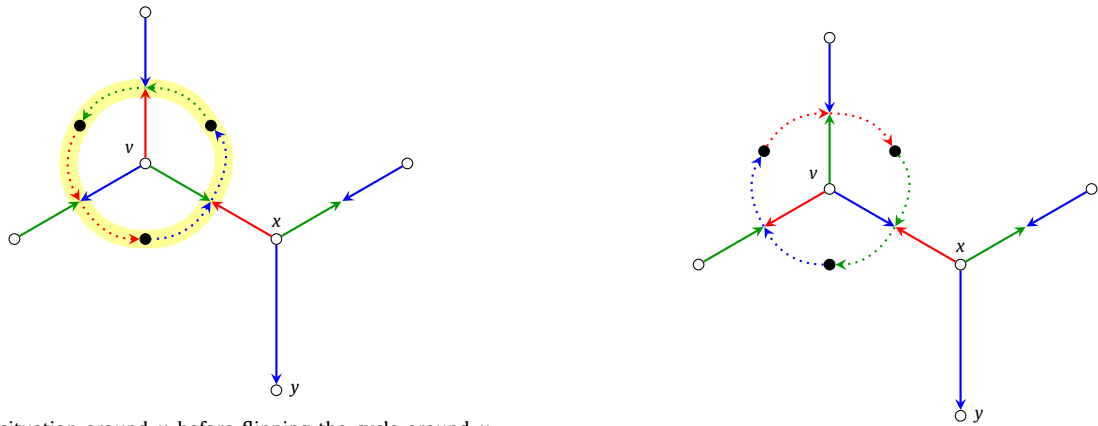


Fig. 12. A Type-A vertex v with its Type-A-neighborhood $N^A(v)$. Vertices of $N^A(v)$ are depicted in yellow.



(i) The situation around v before flipping the cycle around v (marked in yellow).

(ii) The situation around v after flipping the cycle around v .

Fig. 13. Flipping the cycle around the vertex v does not decrease the number of singletons.

Lemma 19. Let G be a planar 3-connected graph and S be its minimal Schnyder wood. Let v be a Type-A vertex of degree 3 with $|N^A(v)| = 3$. Then there exists a counterclockwise cycle C as depicted in Fig. 13i. We refer to C as the cycle around v . For every $x \in N^I(v)$, flipping C does not decrease $m(x)$ (see Fig. 13).

Proof. Let x be a vertex in $N^I(v)$ and suppose w.l.o.g. that x is connected to v by the 1-2-colored edge. Flipping C changes the colors of vx and it becomes 1-3-colored, see Fig. 12 and 13. Observe that, as $|N^A(v)| = 3$, there are exactly two Type-A vertices in $N^I(x)$ by Lemma 18(c).

Consider the edge xy that is outgoing 3-colored at x (Fig. 13). If xy is 1-3-colored, then x is incident to a 1-3-colored edge before and after the flip. So, before and after the flip, x is not a singleton in $\mathcal{P}^{3,1}$. The outgoing 2-colored edge at x is not changed by the flip. The outgoing 1-colored edge at x is 1-2-colored before the flip and 1-3-colored after the flip. So if the outgoing 2-colored edge at x is 1-2-colored, then before and after the flip x is a singleton only in $\mathcal{P}^{2,3}$. And if the outgoing 2-colored edge at x is not 1-2-colored, then it is unidirected by Lemma 14. Thus, before the flip, x is a singleton only in $\mathcal{P}^{2,3}$ and afterwards it is a singleton in $\mathcal{P}^{2,3}$ and $\mathcal{P}^{1,2}$. So $m(x)$ does not decrease.

If xy is not 1-3-colored, then $y \notin N^I(x)$ or y is not Type-A. As observed at the beginning of the proof, there are two Type-A vertices in $N^I(x)$. And hence, the edge leaving x in color 2 needs to be 2-3-colored. So, before and after flipping C , x is a singleton in exactly one compatible ordered path partition. See Fig. 13 for illustration. Thus, also in this case $m(x)$ does not decrease. And hence, for every $x \in N^I(v)$, flipping C does not decrease $m(x)$. \square

Theorem 20. Every 3-connected planar graph G admits a Schnyder wood such that

$$\sum_{i=1}^3 |\{v \mid v \text{ is a singleton in } \mathcal{P}^{i,i+1}\}| \geq \frac{19n}{31} \geq 0.6129 \cdot n.$$

Proof. The proof basically uses the same arguments as in the proof of Theorem 15. We simply improve one counting argument. In the proof of Theorem 15, we use the minimal Schnyder wood. Remember that for every Type-A vertex v every vertex in $N^l(v)$ is a singleton in either one or two of the compatible ordered path partitions. In the proof of Theorem 15, we show that

$$\begin{aligned} \sum_{i=1}^3 s_i &\geq |\{x \in V(G) \mid x \in N^l(v) \text{ for a Type-A vertex } v.\}| \\ &\geq \frac{3}{2} \cdot |\{v \in V(G) \mid v \text{ is Type-A}\}|. \end{aligned}$$

We observe that for a Type-A vertex v every vertex $x \in N^l(v)$ contributes $1/2$ to $3/2 \cdot |\{v \in V(G) \mid v \text{ is Type-A}\}|$. So if a vertex $x \in N^l(u) \cap N^l(w)$ for two Type-A vertices $u \neq w$, then it contributes 1 to $3/2 \cdot |\{v \in V(G) \mid v \text{ is Type-A}\}|$. So we have

$$\frac{3}{2} \cdot |\{v \in V(G) \mid v \text{ is Type-A}\}| = \sum_{x \in V(G)} m'(x)$$

with

$$m'(x) = \begin{cases} 1 & \text{if } x \in N^l(u) \cap N^l(w) \text{ for two Type-A vertices } u \neq w, \\ 1/2 & \text{if } x \in N^l(u) \text{ for exactly one Type-A vertex } u, \\ 0 & \text{otherwise.} \end{cases}$$

In the following proof, we will determine a constant $c = 1/12$ such that

$$\sum_{i=1}^3 is_i \geq \left(\frac{3}{2} + c\right) \cdot |\{v \in V(G) \mid v \text{ is Type-A}\}|.$$

Observe that we take the multiplicity of the singletons into account, i.e. we consider is_i instead of s_i . Our strategy is to start with the counting argument of the proof of Theorem 15, i.e. every vertex x contributes $m'(x)$ to our count. Then we consider the Type-A vertices one by one. For each Type-A vertex v , we search for a vertex x with $m(x) > m'(x)$ that is close to v , i.e., the actual multiplicity of x is higher than the contribution of x to $\sum_{x \in V(G)} m'(x)$. Then we spread $m(x) - m'(x)$ among Type-A vertices that are close to v . If we cannot find such a vertex x close to v , we show that we can locally change the Schnyder wood such that the overall singleton count $\sum_{w \in V(G)} m(w)$ increases. Again, we spread the surplus among Type-A vertices that are close to v .

So we start with the minimal Schnyder wood S of G and perform the counting argument as in Theorem 15. We obtain that

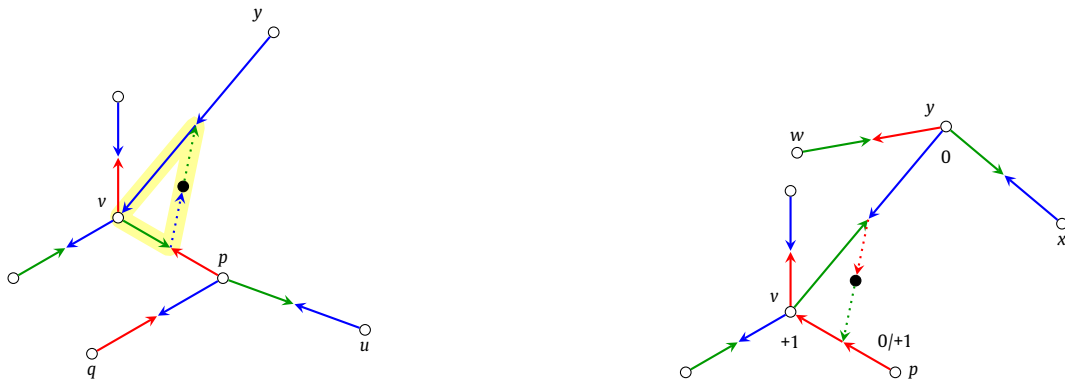
$$\sum_{i=1}^3 is_i \geq \sum_{i=1}^3 s_i \geq \frac{3}{2} \cdot |\{v \in V(G) \mid v \text{ is Type-A}\}|.$$

For every Type-A vertex v , initialize $c(v) = 0$. Refer to $c(v)$ as the *additive* of v . We realize the spreading of the surplus by increasing $c(v)$ for the respective vertices. So we want to achieve that $c(v) \geq 1/12$ for every Type-A vertex of S . Throughout the proof, we refer for a vertex v of G by $N_S^l(v)$ and $N_S^A(v)$ to $N^l(v)$ and $N^A(v)$ with respect to the minimal Schnyder wood S , respectively.

We start by considering the Type-A vertices v that have at least one neighbor $x \in N^l(v)$ such that there is only one Type-A vertex in $N^l(x)$. Since every vertex x' in $N^l(v)$ has at most two Type-A vertices in $N^l(x')$ by Lemma 18(a) and x has only one Type-A vertex in $N^l(x)$, we obtain that this set of Type-A vertices is exactly the set of the Type-A vertices with $|N^A(v)| \leq 2$. Denote this set of Type-A vertices by B and say that x is *bound* to v by Case 0. For such a neighbor x we have $m'(x) = 1/2$ but $m(x) \geq 1$, and hence $m(x) - m'(x) \geq 1/2$. We increase $c(v)$ by $1/12$ and for every $w \in N_S^A(v)$ we increase $c(w)$ by $1/(3 \cdot 12)$. This way, the amount that we spread is at most $1/6$. In the following, we refer to this as *increasing the additive around* v . Hence, if we increase the additive around a vertex a in the remainder of the proof, we perform exactly those changes for $c(a)$ and $c(w)$ for $w \in N_S^A(a)$.

Now, consider the Type-A vertices in $V(G) \setminus B$ that have degree at least four. Initialize $D_{\geq 4}$ to be this set of Type-A vertices. Then, for $v \in D_{\geq 4}$, there is w.l.o.g. an ingoing 3-colored edge vy such that the next edge in clockwise direction around v is bidirected, see Fig. 14i. Observe that, in this case, there is a counterclockwise cycle C in G_S , which is marked yellow in Fig. 14i. Now, proceed iteratively for vertices v in $D_{\geq 4}$. Initialize $F = \emptyset$. Vertices in F will not be considered in Case 3. We use this set in order to assure that certain configurations cannot apply later on in the proof.

Case 1 Assume that $N_S^l(y)$ contains at most one Type-A vertex of S . Then, $m'(y) \leq 1/2$ by the Definition of m' . But, since y has a unidirected outgoing edge it is a singleton in at least one compatible ordered path partition (Fig. 5). Hence, $m(y) \geq 1$ and we obtain that $m(y) - m'(y) \geq 1/2$. We found a vertex y that is close to v such that $m(y) - m'(y) \geq 1/2$.



(i) A Type-A vertex v with degree at least 4. The counterclockwise cycle is marked in yellow.

(ii) The situation in Case 2. The numbers next to the vertices indicate how the multiplicity of the vertices changes.

Fig. 14. The situation around v as in Case 1 and 2 in the proof of Theorem 20.

As we have this surplus which we can spread we do not need to locally change the Schnyder wood. Hence, in this case there is no need to flip C . We increase the additive around v , i.e., as defined above, we increase $c(v)$ by $1/12$ and for every $w \in N_S^A(v)$ we increase $c(w)$ by $1/(3 \cdot 12)$. The amount that we spread is at most $1/6$ in total. Finally, add v to F and delete it from $D_{\geq 4}$. We say y is bound to v by Case 1.

Case 2 Assume that $N_S^l(y)$ contains two Type-A vertices of S . Let yx be the outgoing 2-colored edge at y . Since $N_S^l(y)$ contains two Type-A vertices and the outgoing 3-colored edge of y is unidirected, we know that the endvertices of the other two outgoing edges of y need to be of Type-A and those edges need to be bidirected. Hence, x is of Type-A and the edge yx is incoming 2-colored at x and bidirected. By the definition of Type-A vertices we know that there is only one such edge incident to x . This edge is 2-3-colored. Let vp be the 2-1-colored edge at v . Observe that flipping C increases the total number of singletons by at least one. The edge vy becomes 2-3-colored and the edge vp becomes 1-colored. In the following we show that $m(y)$ does not change, $m(v)$ increases by 1 and $m(p)$ does not decrease, see Fig. 14ii for illustration. Remember that a vertex is a singleton in $\mathcal{P}^{i,i+1}$ if and only if it is not incident to an $i-(i+1)$ -colored edge.

The only edge incident to y that is changed by the flip of C is the edge vy . Before the flip vy is unidirected 3-colored and after the flip it is 2-3-colored. As y is incident to the 2-3-colored edge yx before the flip of C , we know that y is incident to a 2-3-colored edge before and after the flip of C . Hence, it is not a singleton in $\mathcal{P}^{2,3}$ before and after the flip. The other edges incident to y do not change. Hence, for the other compatible ordered path partitions $\mathcal{P}^{1,2}$ and $\mathcal{P}^{3,1}$ y is a singleton after the flip of C if and only if y was a singleton before. Thus, $m(y)$ does not change.

Consider v . Before the flip v is incident to a 1-2-colored, a 2-3-colored and a 3-1-colored edge. Therefore, v is not a singleton in any of the compatible ordered path partitions before the flip of C and hence, $m(v) = 0$ before the flip of C . After the flip v is incident to a 2-3-colored and a 3-1-colored edge but not to a 1-2-colored edge. Hence, v is a singleton in $\mathcal{P}^{1,2}$ but not in $\mathcal{P}^{2,3}$ and $\mathcal{P}^{3,1}$ after the flip of C . Thus, $m(v) = 1$ after the flip of C . And we obtain that $m(v)$ increases by 1.

Let us consider p . The only edge incident to p that is changed by the flip of C is vp . It is 1-2-colored before the flip of C and unidirected 1-colored after the flip of C . Hence, p is not a singleton in $\mathcal{P}^{1,2}$ before the flip and p is a singleton in $\mathcal{P}^{1,2}$ after the flip if and only if it is not incident to a 1-2-colored edge that is different from vp . Also, since vp is the only edge incident to p that is changed by the flip of C , p is a singleton in $\mathcal{P}^{2,3}$ and $\mathcal{P}^{3,1}$ before the flip of C if and only if p is a singleton in $\mathcal{P}^{2,3}$ and $\mathcal{P}^{3,1}$ after the flip, respectively. Hence, $m(p)$ either increases by 1 or does not change, i.e., $m(p)$ does not decrease.

So $m(y)$ does not change, $m(v)$ increases by 1 and $m(p)$ does not decrease. Hence, we flip C and thus obtain a changed Schnyder wood. Say y is bound to v by Case 2.

Let pu be the outgoing 2-colored edge in S at p and let pq be the outgoing 3-colored edge at p (Fig. 14i). Let yw be the outgoing 1-colored edge at y (Fig. 14ii). Now, we need to assure that the change in the Schnyder wood does not affect our future operations, i.e., the operations that we perform for the remaining vertices in $D_{\geq 4}$ and the vertices in $V(G) \setminus (B \cup F)$. In order to achieve this, we add the vertices in $\{v, w, x, u, q\}$ that are Type-A in S to F and delete them from $D_{\geq 4}$. Remember that vertices in F will not be considered in Case 3. We now argue why we need to add exactly those vertices to F and delete them from $D_{\geq 4}$.

Deleting v from $D_{\geq 4}$ assures for every Type-A vertex of S in $D_{\geq 4}$ that the incident edges were not affected by flipping C . Now, consider the Type-A vertices that remain in $V(G) \setminus (B \cup F)$ after having processed $D_{\geq 4}$. They are then considered in Case 3. Adding v to F assures that for every Type-A vertex of S in $V(G) \setminus (B \cup F)$ the incident edges were not affected by flipping C . If q and u are both of Type-A and qp and up are colored as in Fig. 14i, then $p \in N_S^l(q) \cap N_S^l(u)$ and flipping C did change an edge incident to p . In Case 3, we consider pairs of Type-A vertices $a, b \in V(G) \setminus (B \cup F)$ together with a vertex $z \in N_S^l(a) \cap N_S^l(b)$, and we want that the now changed Schnyder wood coincides locally at a, b and z with the

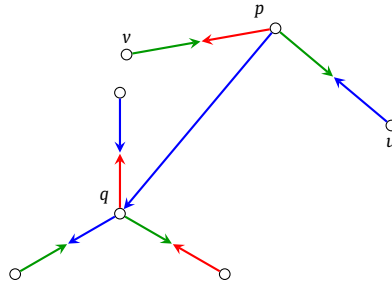


Fig. 15. The situation around q if p was bound to q by Case 2 in the proof of Theorem 20.

minimal Schnyder wood, i.e., the orientation and coloring of the edges incident to a , b and z coincides. Since we add v to F this holds for the edges incident to a and b . But as observed, p , q and u form such a triple and the edge vp is incident to p and flipping C changes the orientation and coloring of vp . Hence, we add the Type-A vertices of $\{q, u\}$ to F . For the same reason, we add the Type-A vertices in $\{w, x\}$ to F . The vertices p and y can each be contained in at most one such triple by Lemma 18(a). Since vy and vp are the only edges changed by flipping C , those two triples are the only such triples. Thus, this assures that for every pair a and b of Type-A vertices of S in $V(G) \setminus (B \cup F)$ and every vertex $z \in N_S^l(a) \cap N_S^l(b)$, the incident edges of z were not affected by flipping C . The following observation becomes important later in the proof (Situation 3).

Observation 1. Since we delete the Type-A vertices of $\{w, x, q, u\}$ from $D_{\geq 4}$, p cannot be bound by Case 2 and y cannot be bound by Case 2 to a vertex other than v .

Consider y . By deleting the Type-A vertices of $\{w, x, q, u\}$ from $D_{\geq 4}$, we delete all Type-A vertices from $D_{\geq 4}$ that are joined to y with an edge that is outgoing at y . If y is bound to a Type-A vertex by Case 2, this vertex is joined to y with an edge that is outgoing at y . Thus, y is not bound to any other Type-A vertices by Case 2.

Now, we show the statement for p . Assume, for the sake of contradiction, that p is bound by Case 2. Let w.l.o.g. p be bound to q . Then pq is unidirected and incoming 3-colored at q such that the next edge in clockwise order is bidirected and u and q are Type-A by the requirements of Case 2 (Fig. 15). Since we delete the Type-A vertices of $\{w, x, q, u\}$ from $D_{\geq 4}$, q has been considered before v . Hence, at the time we considered q , the Type-A vertex v was still in $D_{\geq 4}$. But, observe that after treating q we delete by our procedure for Case 2 the Type-A vertices of the set $\{v, u\}$ from $D_{\geq 4}$ as vp and pu are the outgoing 1- and 2-colored edges at p , respectively (Fig. 15). As v is a Type-A vertex it is deleted from $D_{\geq 4}$, contradicting the fact that we consider it after q . Hence, p cannot be bound by Case 2.

Finally, for every Type-A vertex z in $\{v, u, q, w, x\}$ we increase the additive around z , i.e., as defined above, we increase $c(z)$ by $1/12$ and for every $w \in N_S^A(z)$ we increase $c(z)$ by $1/(3 \cdot 12)$. The amount that we spread is at most $5/6$ in total.

For the remaining Type-A vertices, we again proceed iteratively. So let $v \in V(G) \setminus (B \cup F)$ be Type-A. We have that v is of degree three and that every vertex $a \in N_S^l(v)$ has two neighbors in $N_S^l(a)$ that are Type-A vertices, i.e. $|N_S^A(v)| = 3$, since we considered the other Type-A vertices in the previous cases. If $N_S^A(v) \setminus (B \cup F) = \emptyset$, we simply add v to F , say we skip v . Later on we show that for vertices that we skipped we already increased the additive sufficiently. Otherwise, there is a vertex $w \in N_S^A(v) \setminus (B \cup F)$. As $w \in N_S^A(v) \setminus (B \cup F)$, w is of degree 3 and $|N_S^A(w)| = 3$.

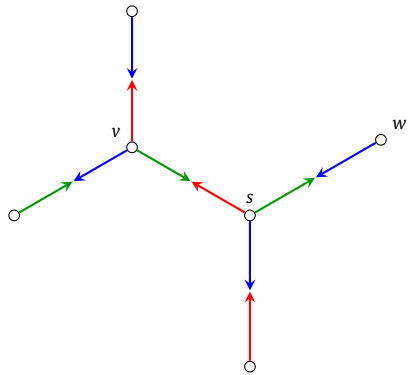
As $w \in N_S^A(v)$, there is a vertex $s \in N_S^l(v) \cap N_S^l(w)$. W.l.o.g. we may assume that s is connected to v by a 1-2-colored edge and to w by a 2-3-colored edge. As we can observe in Fig. 16, the outgoing 3-colored edge of s is neither incident to v nor to w . The following case distinction is by the colors of this edge (Fig. 16).

Case 3.1 s has an edge that is outgoing 3-colored and ingoing 1-colored. Then, there is a configuration around s which cannot occur due to Lemma 14, see Fig. 16i.

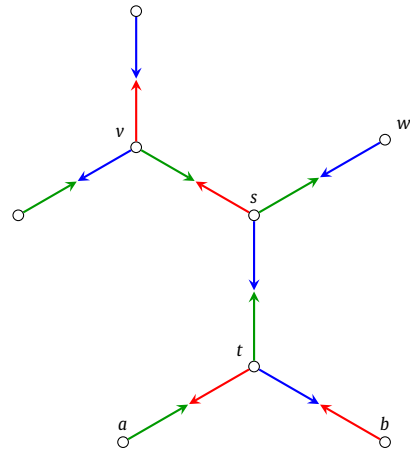
Case 3.2 s has an edge st that is outgoing 3-colored and ingoing 2-colored. Then, by Lemma 14, $N_S^l(t)$ cannot contain two Type-A vertices, see Fig. 16ii. As for vertices that are bound by Case 0, we obtain that $m(t) - m'(t) \geq 1/2$. We increase the additive around v and add v to F . Say t is bound to v by Case 3.2.

Case 3.3 s has an unidirected outgoing 3-colored edge. Observe that s is incident to a 1-2-colored and a 2-3-colored edge but not to a 3-1-colored edge. Hence, s is a singleton in exactly one compatible ordered path partition. Observe that, since w is a Type-A vertex of degree 3, there is a counterclockwise cycle C' around w . After flipping C' the edge sw is 2-1-colored (Fig. 16iv). For an illustration of such a flip we refer the reader to Fig. 13. Hence, after flipping C' , s is incident to two 1-2-colored edges and no 2-3-colored and 3-1-colored edge. Thus, s is a singleton in two ordered path partitions and flipping C' increases $m(s)$ by 1, see Fig. 16iii and 16iv.

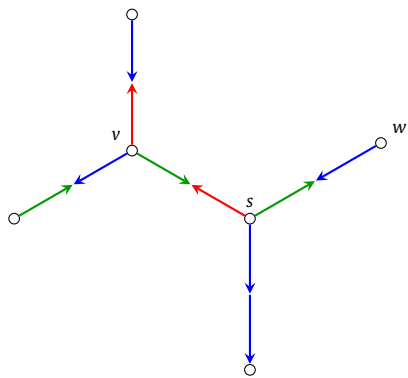
Now, we show that this flip increases the overall singleton count. This flip only changes the coloring and orientation of edges that join vertices of $N^l(w)$ with w . Hence, for a vertex not in $N^l(w) \cup \{w\}$ the multiplicity does not change. For w itself, we observe that it is incident to a 1-2-colored, a 2-3-colored and a 3-1-colored edge before and after the



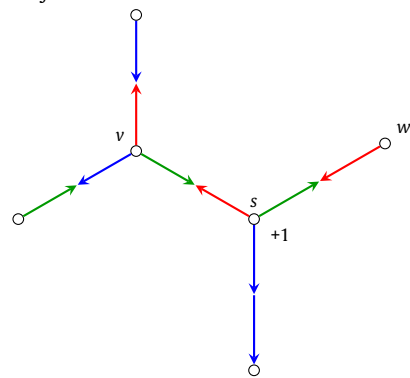
(i) In Case 3.1 the situation around s is forbidden by Lemma 14.



(ii) If in the situation of Case 3.2 t has two Type-A vertices a and b in $N^I(t)$, we have a configuration around t which is forbidden by Lemma 14.



(iii) The situation in Case 3.3.



(iv) The situation in Case 3.3 after flipping the cycle C' around w . The multiplicity of s increases by 1.

Fig. 16. The situation around v as in Case 3 of the proof of Theorem 20.

flip, compare Fig. 13. Hence, $m(w) = 0$ before and after the flip. By Lemma 19, we also obtain that for each vertex in $N^I(w)$ flipping C' does not decrease the multiplicity. As observed above, flipping C' increases $m(s)$ by 1. Hence, flipping C' increases the overall singleton count by 1.

Therefore, we flip the cycle C' . For every $q \in N_S^A(w)$, we increase the additive around q . Observe that since $|N_S^A(w)| = 3$, $c(w)$ increases by $3 \cdot 1/(3 \cdot 12) = 1/12$. The amount that we spread is at most $3/6$. Add $w \cup N_S^A(w)$ to F . Say s is bound by Case 3.3 to w .

Now, we need to show that this process implies the constant $c = 1/12$. The additive is at least $1/12$ for every Type-A vertex in B and for every Type-A vertex which we added to F in Cases 1, 2, 3.2 and 3.3.

Consider the Type-A vertices that we skipped. Assume, for the sake of contradiction, that there are two Type-A vertices a and b that we skipped such that $a \in N_S^A(b)$ (this directly implies that $b \in N_S^A(a)$). W.l.o.g. we skipped a before b . Then, at the moment we skipped a in our procedure b has not yet been added to F . Hence, $N_S^A(a) \setminus (B \cup F)$ contains b and thus, is non-empty. This contradicts the fact that we skipped a . Therefore, the Type-A-neighborhood of a Type-A vertex that we skipped does not contain another Type-A vertex that we skipped. Hence, we have that for a Type-A vertex w that we skipped there are three vertices in $N_S^A(w)$ and we increased the additive around each of those three. Thus, $c(w) \geq 3 \cdot 1/(3 \cdot 12) = 1/12$. Hence, we indeed have $c(v) \geq 1/12$ for every Type-A vertex v .

It is left for us to show that if a vertex is bound to multiple Type-A vertices, then the surplus that we have at that vertex suffices for each of the Type-A vertices. So let x be some vertex that is not of Type-A. The following three situations might occur.

Situation 1 Assume $x = s$ is bound to w by Case 3.3. We show that s is not bound to any other vertex. There are two Type-A vertices in $N_S^I(s)$ (v and w in Fig. 16iii), so s cannot be bound by Case 0, 1, or 3.2, since in those cases $N_S^I(s)$ contains at most one Type-A vertex. If s was bound by Case 2, then w would have been added to F in Case 2. Hence, it would

not have been available for Case 3.3, a contradiction. So s is bound only by Case 3.3. Observe that s cannot additionally be bound by Case 3.3 to a vertex different from w since we add both Type-A vertices in $N_S^l(s)$ to F in Case 3.3. We have $m'(s) = 1$ and $m(s) = 1$. But, by flipping the cycle C' , we increase the total number of singletons by at least one in Case 3.3. The sum of the additives is increased by at most $3/6$ in Case 3.3. Thus, our counting works in this situation.

Situation 2 Assume x is bound to v by Case 0, Case 1 or Case 3.2. In Case 0, Case 1 and Case 3.2, x has at most one Type-A vertex in $N_S^l(x)$. So x cannot be bound by Case 2 or Case 3.3, since in those cases there are two Type-A vertices in $N_S^l(x)$. The remaining cases are Case 0, Case 1 and Case 3.2.

We show that x can be bound to at most three different Type-A vertices in total. Observe that xv is outgoing at x (uni- or bidirected) if x is bound to a Type-A vertex v by Case 0 or Case 1. If $x = t$ is bound to w by Case 3.2, we have a path consisting of $x = t$, s and w such that ts is outgoing i -colored at t , s is not a Type-A vertex and sw is outgoing i -colored at s , for some $i \in \{1, 2, 3\}$ (Fig. 16ii). Since x has exactly three outgoing edges by Definition 1(c), the above facts yield that x is bound to at most three different Type-A vertices.

In each of those three Case 0, Case 1 and Case 3.2, the increase of the additive is at most $1/6$. Thus, in this situation the additive is increased by at most $3/6$ in total. As $m(t) - m'(t) \geq 1/2 = 3/6$ in Case 0, Case 1 and Case 3.2, our counting argument is correct in this situation.

Situation 3 Assume $x = y$ is bound by Case 2 to a Type-A vertex v . As observed in Situation 1, y cannot be bound by Case 3.3. Also, as observed in Observation 1 of Case 2, y cannot be bound by Case 2 to an additional vertex different from v . And, as observed in Situation 2, y cannot be bound by Case 0, Case 1 or Case 3.2. By flipping the cycle C in Case 2, the total number of singletons increases by at least 1. We increase the sum of the additives by at most $5/6$. So our counting is correct.

This situation distinction shows that our counting argument is indeed correct. So we have with the same arguments as in the proof of Theorem 15 that

$$\begin{aligned} \sum_{i=1}^3 is_i &\geq \left(\frac{3}{2} + \frac{1}{12}\right) \cdot |\{v \in V(G) \mid v \text{ is Type-A}\}| = \frac{19}{12} \left(n - \sum_{i=1}^3 s_i\right) \\ &\geq \frac{19}{12} \left(n - \sum_{i=1}^3 is_i\right) \\ \Rightarrow \sum_{i=1}^3 is_i &\geq \frac{19}{31}n. \end{aligned}$$

Since $\sum_{i=1}^3 |\{v \mid v \text{ is a singleton in } \mathcal{P}^{i,i+1}\}| = \sum_{i=1}^3 is_i$, the claim follows. \square

4. Leaves

Let T_1, T_2 and T_3 be the three trees of a Schnyder wood. By l_i we denote the number of leaves of the tree T_i . In this section, we consider the number of leafs of the trees of a Schnyder wood. We show that $\sum_{i=1}^3 l_i \geq (3n + 6)/5$ for the minimal Schnyder wood of a 3-connected planar graph of order n . We also give a sequence of graphs that shows that this bound and the bound of Theorem 15 are tight.

Lemma 21. *Let G be a 3-connected planar graph and let S be a minimal Schnyder wood of G . If a vertex $v \in V(G)$ has an edge that is outgoing i -colored and ingoing $(i + 1)$ -colored, then v is a leaf in T_i or T_{i+2} .*

Proof. W.l.o.g. let v be such that it has an edge that is outgoing 1-colored and ingoing 2-colored. Assume, for the sake of contradiction, that v is neither a leaf in T_1 nor in T_3 . Then it has an ingoing 3-colored edge e . If e is undirected, then there is a clockwise cycle in S , see Fig. 10iii. This contradicts the minimality of S . So e is also outgoing 2-colored at v . Now, symmetric arguments show that the at v ingoing 1-colored edge is 1-3-colored. This contradicts Lemma 14. So v is a leaf in T_1 or T_3 . \square

Theorem 22. *Let G be a 3-connected planar graph and let S be a minimal Schnyder wood of G . Then*

$$\sum_{i=1}^3 l_i \geq \frac{3n + 6}{5}.$$

Proof. For technical reasons, we assume w.l.o.g. that $l_1 \geq l_2, l_3$. Denote the compatible ordered path partition given by the maximal 2-3-colored paths by $\mathcal{P}^{2,3} = (P_0, \dots, P_s)$. We define $a, b, c : V(G) \rightarrow \{0, 1\}$ in the following. Those functions help us to give a bound on $n = |V(G)|$ in terms of the number of leaves. Recall that $V_k = \bigcup_{i=0}^k V(P_i)$, as in Definition 11.

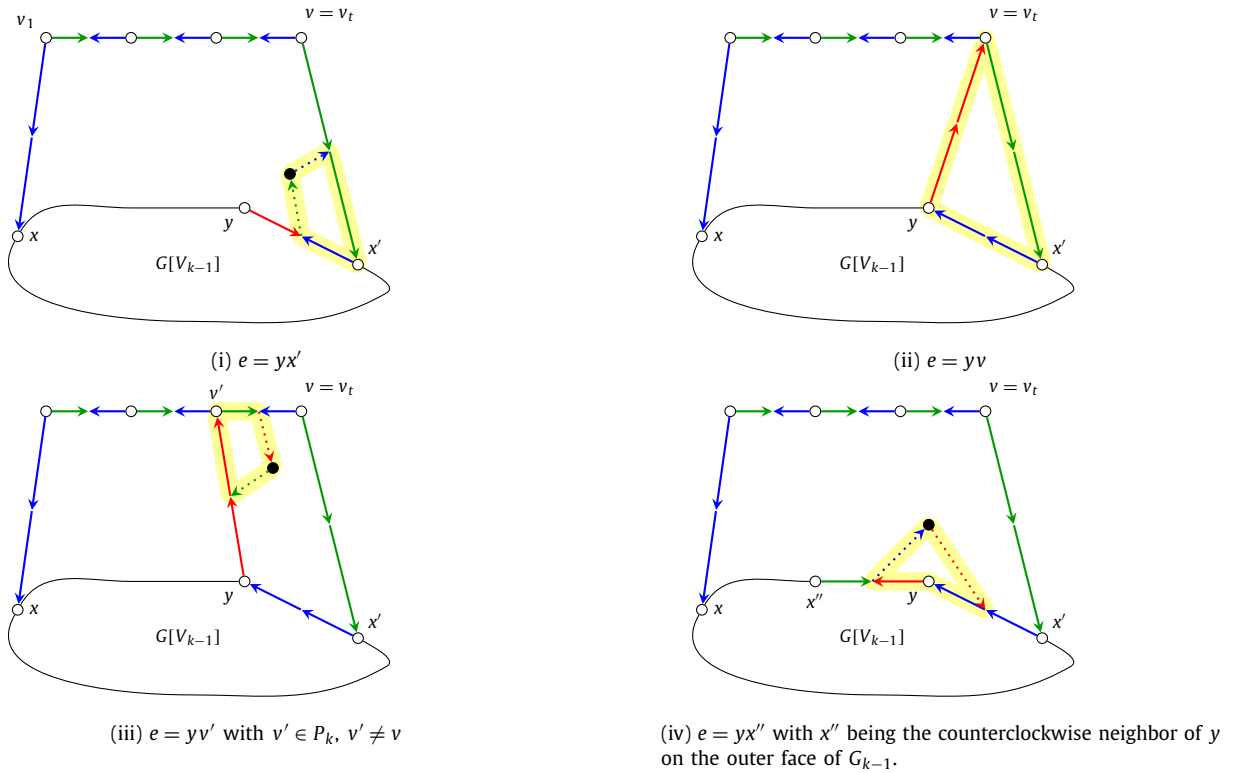


Fig. 17. If $v = v_t$ is connected to x' by a 2-colored edge, then we always find a clockwise cycle. Remember that x' is a leaf in the 2-colored tree on $G[V_{k-1}]$.

In this proof, we exploit that we can count the number of leaves of a tree T_i in two different ways. One way is to directly count the leaves. The other way is to count the in-degree for every vertex v that is not a leaf, i.e. the number of edges that are ingoing at v . Denote by $\text{deg}_i^{\text{in}}(v)$ the number of ingoing i -colored edges at v , for $i \in \{1, 2, 3\}$. We obtain that

$$1 + \sum_{\substack{v \in V(G), \\ v \text{ is not a leaf of } T_i}} (\text{deg}_i^{\text{in}}(v) - 1) = l_i.$$

Let $\{v_1, \dots, v_t\} = P_k \in \mathcal{P}^{2,3}$ for some $k \in \{0, \dots, s\}$ such that v_i appears before v_{i+1} in clockwise order around the outer face of $G[V_k]$ for all $i \in \{1, \dots, t-1\}$. If $P = P_0$, order P such that $v_1 = r_3$ and $v_t = r_2$. For a vertex $v \in P_k$, we define the value of a , b and c in the following.

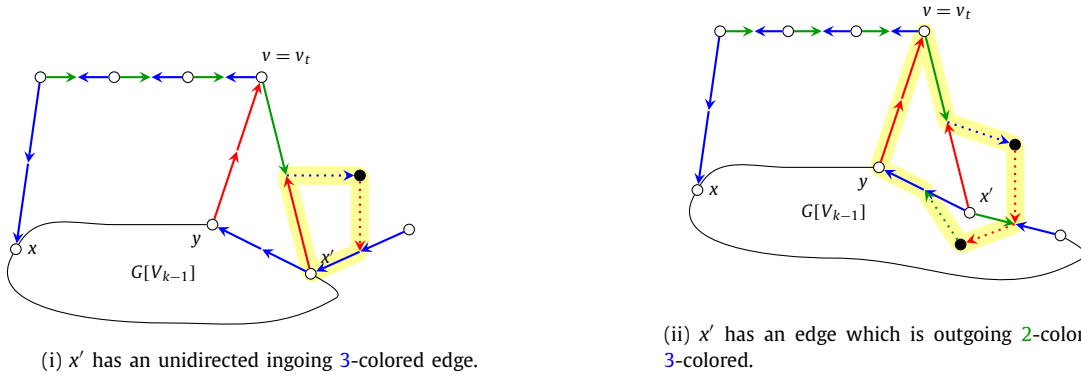
- Case 1** $v = v_i$ for some $i \in \{1, \dots, t-1\}$ or $v = r_2$. Then v has an edge that is outgoing 2-colored and ingoing 3-colored or $v = r_2$. So v is a leaf in T_2 or T_1 , by Lemma 21, or $v = r_2$ is a leaf in T_1 . We define $a(v) = 1$ and $b(v) = c(v) = 0$.
- Case 2** $v = v_t$ and $v \neq r_2$. Then v has an outgoing 2-colored edge vx' which connects it to $G[V_{k-1}]$. And v_1 has an outgoing 3-colored edge v_1x which connects it to $G[V_{k-1}]$.

Case 2.1 x is not a leaf of the subtree of T_3 or x' is not a leaf of the subtree of T_2 in $G[V_{k-1}]$. Observe that the edges v_1x and vx' increases the in-degree of x in color 3 and the in-degree of x' in color 2, respectively. We define $b(v) = 1$ and $a(v) = c(v) = 0$.

Case 2.2 The vertices x and x' are both a leaf of the subtree of T_3 and T_2 in $G[V_{k-1}]$, respectively. The edge vx' is either 1-2-colored or it is unidirected 2-colored.

We prove that vx' cannot be unidirected. Assume, for the sake of contradiction, that it has only color 2. The vertex x' has a counterclockwise neighbor y on the outer face of $G[V_{k-1}]$. This neighbor has an outgoing 1-colored edge e . There are four different possibilities for e either $e = yx'$, $e = yv$, $e = yv'$ with $v' \in P_k$ and $v' \neq v$ or $e = yx''$ with x'' being the counterclockwise neighbor of y on the outer face of $G[V_{k-1}]$. In all four cases, there is a clockwise cycle in \tilde{G}_S , see Fig. 17. So vx' is 1-2-colored and x' is a leaf in T_1 or T_3 , by Lemma 21.

Furthermore, the clockwise cycles in Fig. 17iii and 17iv do not depend on the coloring of vx' . So even if vx' is 1-2-colored, only $e = yv$ and $e = yx'$ is possible. If $e = yx'$, then x' is not a leaf in T_1 and hence it is a leaf in T_3 . If $e = yv$, then x' is also a leaf in T_3 since otherwise we obtain a clockwise cycle in \tilde{G}_S , see Fig. 18. So in any case x' is a leaf in T_3 . We set $c(v) = 1$ and $a(v) = b(v) = 0$.



(i) x' has an unidirected ingoing 3-colored edge.

(ii) x' has an edge which is outgoing 2-colored and ingoing 3-colored.

Fig. 18. Here vx' is 1-2-colored and $e = yv$. If x' is not a leaf in T_3 , then it is a leaf in T_1 by Lemma 21 and we find a clockwise cycle.

For every vertex v , we either have $a(v) = 1, b(v) = 1$ or $c(v) = 1$. Thus, we obtain that $n = \sum_{v \in V(G)} (a(v) + b(v) + c(v))$. Furthermore, observe that $a(v) = 1$ if and only if Case 1 applies. In Case 1, v is a leaf in T_1 or T_2 . So $\sum_{v \in V(G)} a(v) \leq l_1 + l_2$. Also, $c(v) = 1$ if and only if Case 2.2 applies and in that case x' is a leaf in T_3 . Observe that in Case 2.2 vx' is 1-2-colored such that color 2 is outgoing at v . Hence, the function that maps each vertex v for which Case 2.2 applies to the endpoint of its outgoing 2-colored edge is a bijection. In the description of Case 2.2 this endpoint is called x' . This endpoint is a leaf in T_3 . And hence $\sum_{v \in V(G)} c(v) \leq l_3$. As above, $b(v) = 1$ if and only if Case 2.1 applies. In Case 2.1, we observe that $\deg_3^{\text{in}}(x)$ and $\deg_2^{\text{in}}(x')$ increase. Furthermore, x or x' is not a leaf of the subtree of T_3 or T_2 in $G[V_{k-1}]$, respectively. This gives

$$\sum_{v \in V(G)} b(v) \leq \sum_{\substack{v \in V(G), \\ v \text{ is not a leaf of } T_3}} (\deg_3^{\text{in}}(v) - 1) + \sum_{\substack{v \in V(G), \\ v \text{ is not a leaf of } T_2}} (\deg_2^{\text{in}}(v) - 1).$$

As observed above, this gives

$$\sum_{v \in V(G)} b(v) \leq l_3 - 1 + l_2 - 1.$$

Altogether, we obtain that

$$\begin{aligned} n &= \sum_{v \in V(G)} (a(v) + b(v) + c(v)) = \sum_{v \in V(G)} a(v) + \sum_{v \in V(G)} b(v) + \sum_{v \in V(G)} c(v) \\ &\leq (l_1 + l_2) + (l_3 - 1 + l_2 - 1) + l_3. \end{aligned}$$

By pigeonhole principle, there exists $i \in \{1, 2, 3\}$ such that $l_i \geq (n + 2)/5$. Since $l_1 \geq l_2, l_3$ by the assumption at the beginning of the proof, we have that $l_1 \geq l_i \geq (n + 2)/5$. So we obtain that

$$\begin{aligned} n + 2 &\leq (l_1 + l_2) + (l_2 + l_3) + l_3 \\ \Rightarrow \quad n + 2 + \frac{n + 2}{5} &\leq 2 \sum_{i=1}^3 l_i \\ \Rightarrow \quad \frac{3n + 6}{5} &\leq \sum_{i=1}^3 l_i. \quad \square \end{aligned}$$

Remark. Kindermann et al. [16, Lemma 9] showed that $\sum_{i=1}^3 l_i \leq 2n + 1$. The graph in Fig. 19ii implies that this bound is tight. Observe that this graph does not have oriented cycles, so the Schnyder wood is minimal.

Using pigeonhole principle, Theorem 22 implies the following corollary.

Corollary 23. Let G be a 3-connected planar graph and let S be a minimal Schnyder wood of G . Then, one of the trees of the Schnyder wood has at least $\lceil (n + 2)/5 \rceil$ leaves.

In the following we consider the number of leaves on triangulated planar graphs. A result of Zhang et al. [19] implies that one of the trees of the Schnyder wood has at least $\lceil (n + 1)/2 \rceil$ leaves. In Corollary 24, we are able to show that

there is not only one such tree but at least two. Corollary 25 provides a lower bound on $\sum_{i=1}^3 l_i$. It can be obtained by combining Theorem 1 (2.) and Lemma 4 (1.) of [19]. But, since it follows immediately from the proof of Corollary 24, we give a different proof. The subsequent remark considers the tightness of those bounds known for the number of leaves of triangulated planar graphs, i.e., we give graphs that (almost) attain those bounds. We also argue that the minimality of the Schnyder wood is a necessary condition.

Corollary 24. *Let G be a triangulated planar graph and let S be a minimal Schnyder wood of G . Then there exist $i \neq j \in \{1, 2, 3\}$ such that $l_i, l_j \geq \lceil (n + 1)/2 \rceil$.*

Proof. We only need to observe that in the proof of Theorem 22 some cases cannot occur that often. This implies a bound on $\sum_{v \in V(G)} a(v)$ and $\sum_{v \in V(G)} c(v)$.

Since G is triangulated, only the edges on the outer face are bidirected, by Lemma 4. So there is exactly one vertex that has an edge which is outgoing 2-colored and ingoing 3-colored, namely r_3 . Thus, Case 1 applies to exactly r_3 and r_2 and we have $\sum_{v \in V(G)} a(v) = 2$.

Consider Case 2.2. Here, we show in the proof of Theorem 22 that $v x'$ needs to be 1-2-colored. Since G is triangulated, $v = r_1$ and $x' = r_2$. But, $x' = r_2$ is not a leaf in T_2 . Thus, the condition of Case 2.2 is not met and $v = r_1$ is handled in Case 2.1. So $\sum_{v \in V(G)} c(v) = 0$.

If $v = r_1$, then Case 2.1 applies. Also, we observe that $x' = r_2$ is not a leaf in T_2 and $x = r_3$ is not a leaf in T_3 . The in-degree of x' in color 2 and the in-degree of x in color 3 is increased by the path $P_s = r_1$. On the other hand $\sum_{v \in V(G)} b(v) = 1 + \sum_{v \in V(G) \setminus \{r_1\}} b(v)$. Hence, $\sum_{v \in V(G)} b(v) \leq l_2 - 1 + l_3 - 1 - 1$. In total we obtain

$$n \leq 2 + l_2 - 1 + l_3 - 1 - 1 = l_2 + l_3 - 1.$$

By pigeonhole principle, w.l.o.g. $l_2 \geq \lceil (n + 1)/2 \rceil$. Symmetrically, we obtain that $n \leq l_1 + l_3 - 1$. Thus, l_1 or l_3 is at least $\lceil (n + 1)/2 \rceil$. This proves the claim. \square

Corollary 25. *Let G be a triangulated planar graph and let S be a minimal Schnyder wood of G . Then*

$$\sum_{i=1}^3 l_i \geq \frac{3n + 3}{2}.$$

Proof. As in the proof of Corollary 24, for any $i \neq j \in \{1, 2, 3\}$, we have

$$n \leq l_i + l_j - 1.$$

Summing up gives

$$\begin{aligned} 3n &\leq 2 \sum_{i=1}^3 l_i - 3 \\ \Rightarrow \frac{3n + 3}{2} &\leq \sum_{i=1}^3 l_i. \quad \square \end{aligned}$$

Remark. As mentioned above, Kindermann et al. [16, Lemma 9] showed that $\sum_{i=1}^3 l_i \leq 2n + 1$. Together with this bound, Corollary 25 implies that for triangulated planar graphs of order n with a minimal Schnyder wood we have

$$\frac{3n + 3}{2} \leq \sum_{i=1}^3 l_i \leq 2n + 1.$$

Also, for every $k \geq 2$, there exists a triangulated planar graph H_k on $n = 2k + 3$ vertices with a minimal Schnyder wood such that

$$\begin{aligned} l_1 &= \frac{n + 1}{2}, \\ l_2 = l_3 &= \frac{n + 3}{2}, \\ \sum_{i=1}^3 l_i &= \frac{3n + 7}{2}. \end{aligned}$$

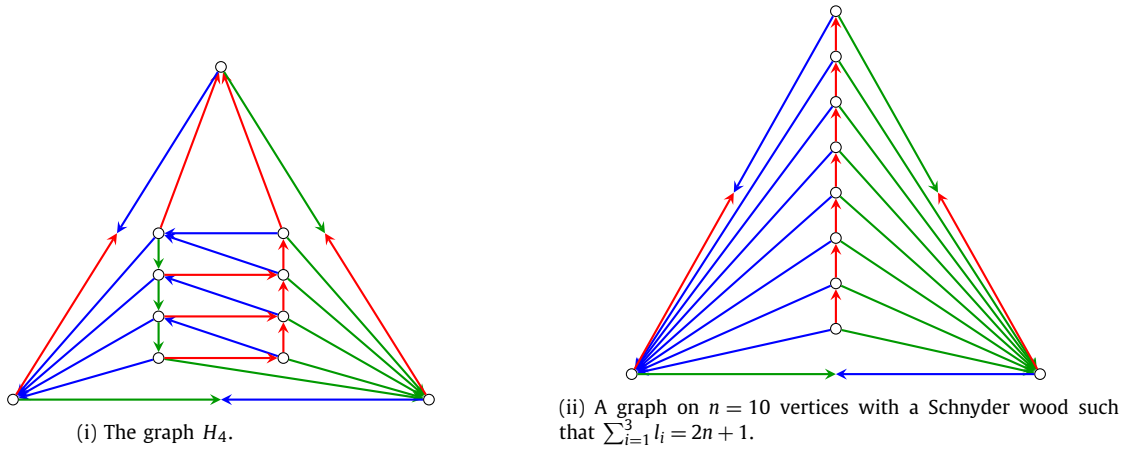


Fig. 19. The graphs that show the tightness of the upper and lower bound on $\sum_{i=1}^3 l_i$ for triangulated planar graphs.

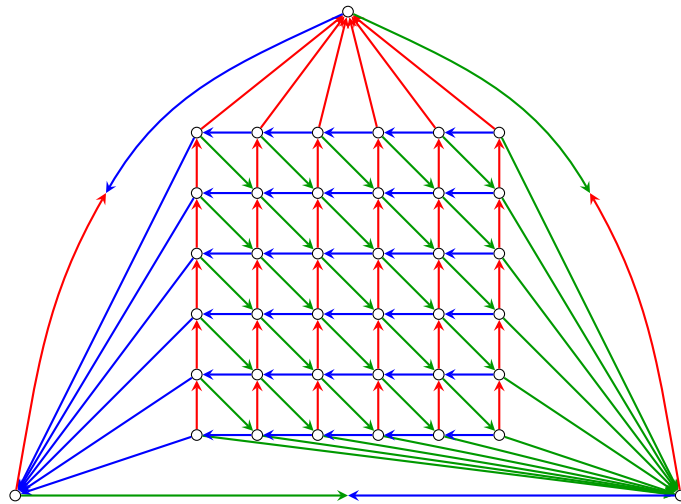


Fig. 20. The graph H'_6 of order 39 with a Schnyder wood such that $l_1 = l_3 = 8$ and $l_2 = 13$.

See Fig. 19i for H_4 . It is easy to see how to construct H_k in general. Thus, the bound of Corollary 25 is tight up to a constant. As stated before, the upper bound is also tight. See Fig. 19ii for illustration. The graph in Fig. 19ii also shows that we cannot give a bound on l_1, l_2 and l_3 simultaneously, as we did in Corollary 24 for two of those.

For Corollary 25, we need the assumption that the Schnyder wood is minimal. For any $k \in \mathbb{N}$, there is a triangulated plane graph H'_k of order $k^2 + 3$ with a Schnyder wood such that $l_1 = l_3 = k + 2$ and $l_2 = 2k + 1$. Obviously, the statement of Corollary 25 does not hold for those graphs. See Fig. 20 for H'_6 . For different k , the graph H'_k and its Schnyder wood can be obtained by adapting the size of the grid.

The next theorem shows that the bounds of Theorem 15 and 22 are both tight.

Theorem 26. *There exists a sequence G_k of graphs and minimal Schnyder woods S_k of G_k such that for arbitrarily chosen ordered path partitions \mathcal{P}_k compatible with S_k , we have*

$$\frac{|\{v \mid v \text{ is a singleton in } \mathcal{P}_k\}|}{|V(G_k)|} \rightarrow \frac{1}{5}, \text{ for } k \rightarrow \infty.$$

Furthermore, for each of the three trees T_1^k, T_2^k and T_3^k of S_k ,

$$\frac{|\{v \mid v \text{ is a leaf in } T_j^k\}|}{|V(G_k)|} \rightarrow \frac{1}{5}, \text{ for } k \rightarrow \infty.$$

This shows that the lower bounds of Theorems 15 and 22 are tight.

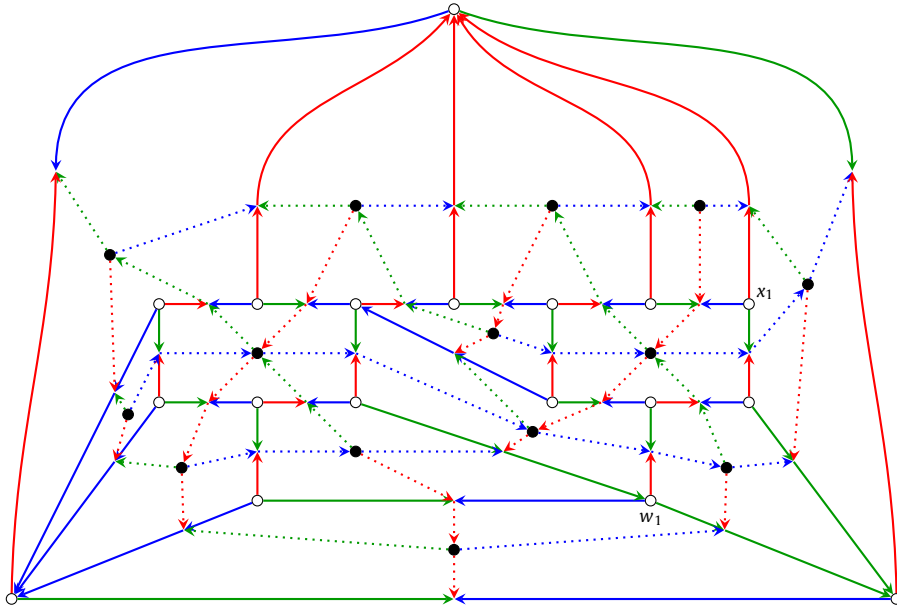


Fig. 21. The completion of the graph G_1 , with its Schnyder wood S_1 . Vertices and edges in the outer face of G_1 are suppressed to enhance readability.

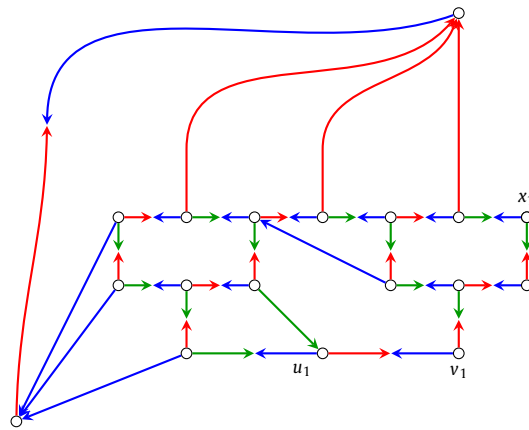


Fig. 22. The graph obtained after the described modifications of G_1 before we add H .

Proof. We define G_k and its Schnyder wood S_k iteratively. Start with G_1 as depicted in Fig. 21. It is easy to verify that S_1 is the minimal Schnyder wood using Lemma 10. Define $w^1, x^1 \in V(G_1)$ as in Fig. 21.

In order to obtain G_2 , we split w_1 into two vertices u_1 and v_1 , i.e. we delete w_1 , introduce new adjacent vertices u_1 and v_1 and connect them as in Fig. 22 to the neighbors of w_1 . Vertex u_1 is connected to all neighbors of w_1 that were connected to w_1 with an undirected ingoing 2-colored edge or a 2-3-colored edge and v_1 is connected only to the neighbor of w_1 that was connected to w_1 with a 1-2-colored edge.

Then we delete r_2 and the edge $x_1 r_1$ (Fig. 22). Let the graph H be as depicted in Fig. 23. We add H with its coloring by identifying the vertices and edges of G_1 and H along the clockwise and counterclockwise path along the outer face from x_1 to u_1 and $x \in V(H)$ to $u \in V(H)$, respectively (see Fig. 24).

We add colored edges and define w_2 and x_2 as depicted in Fig. 24. The graph we obtain is G_2 . Observe the following. If we now delete r_2 and its incident edges, then on the clockwise path on the outer face from r_1 to r_3 the colors appear in the same pattern as on the corresponding path in G_1 . So we can iterate this procedure. That way we to obtain G_k for every $k \in \mathbb{N}$.

We now need to show that the orientation and coloring which we obtain is a Schnyder wood of G_k . We prove this by induction. In G_1 we have a Schnyder wood. In order to see that we have a Schnyder wood in G_k , observe that local requirements of Definition 1, especially (c) and (d), are met for every vertex and face in the subgraph H of G_k . For the faces and vertices that are also in G_{k-1} requirements (c) and (d) hold by induction. When we split w_1 into u_1 and v_1 we change

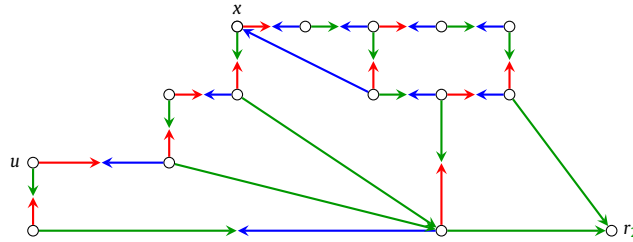


Fig. 23. The graph H with its orientation and coloring.

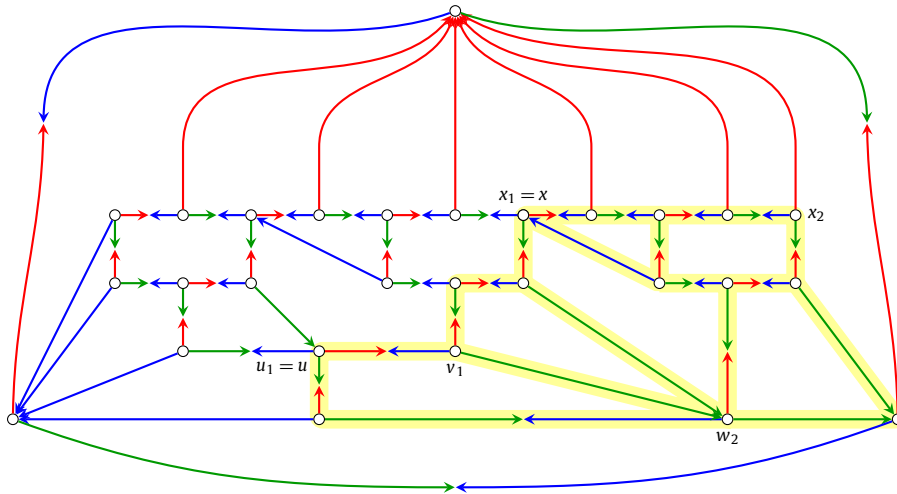


Fig. 24. The graph G_2 , and its Schnyder wood S_2 . The graph H is marked in yellow.

one face of G_{k-1} . Observe that also for this face Definition 1(d) holds. Definition 1(a) and (b) trivially hold. So we do indeed have a Schnyder wood.

In order to see that the resulting Schnyder wood S_k of the graph G_k is minimal, we give an elimination order as in Lemma 10 by induction. It is easy to show that there exists such an order for \widetilde{G}_{1S_1} . In Fig. 25, we gave part of an elimination order of \widetilde{G}_{2S_2} for illustration.

So let $k \geq 2$. We now assign the indices of the elimination order to vertices of \widetilde{G}_{kS_k} starting with the highest and ending with the lowest. The roots of the primal and dual Schnyder wood get the highest indices; call this set of vertices R . The next indices are given to the set C of crossing vertices adjacent to those roots. They satisfy property (a) of Lemma 10. Then the set D of dual vertices that are on the boundary of the graph $\widetilde{G}_{kS_k}[V(\widetilde{G}_{kS_k}) \setminus (R \cup C)]$ follows. Those either satisfy property (a) or (b) of Lemma 10. Next, we have the remaining vertices of H , its crossing vertices and the dual vertices in the interior of H except for u_{k-1} ; call that set A . We eliminate the vertices in A in the same order as shown in Fig. 25. It is easy to verify that this order satisfies the conditions of Lemma 10.

The graph $\widetilde{G}_{kS_k}[V(\widetilde{G}_{kS_k}) \setminus (R \cup C \cup D \cup A)]$ can be found as a subgraph in $\widetilde{G}_{k-1S_{k-1}}$ with the same orientation and coloring of the edges. As S_{k-1} is minimal we have an elimination order on $\widetilde{G}_{k-1S_{k-1}}$ and we can use this order on the vertices of $\widetilde{G}_{kS_k}[V(\widetilde{G}_{kS_k}) \setminus (D \cup C \cup B \cup A)]$ to obtain an elimination order of \widetilde{G}_{kS_k} . Lemma 9 then implies that S_k is indeed minimal.

Now, we calculate the number of singletons of the compatible ordered path partition $\mathcal{P}_k^{i,i+1}$. We explicitly compute the number of singletons in $\mathcal{P}_k^{1,2}$. The number of singletons in $\mathcal{P}_k^{3,1}$ and $\mathcal{P}_k^{2,3}$ follows by similar arguments. The singletons in $\mathcal{P}_k^{1,2}$ are exactly the vertices in G_k that are not incident to a 1-2-colored edge. Observe that there are only two vertices in H that are not incident to a 1-2-colored edge. In Fig. 24, they are the clockwise second and third neighbor of r_1 that is connected to r_1 by a unidirected 1-colored edge. In G_1 there are four vertices that are not incident to a 1-2-colored edge. And thus we obtain that there are $2k + 2$ singletons in $\mathcal{P}_k^{1,2}$. Similar arguments imply that

$$|\{v \mid v \text{ is a singleton in } \mathcal{P}_k^{3,1}\}| = 2k + 4,$$

$$|\{v \mid v \text{ is a singleton in } \mathcal{P}_k^{2,3}\}| = 2k + 2.$$

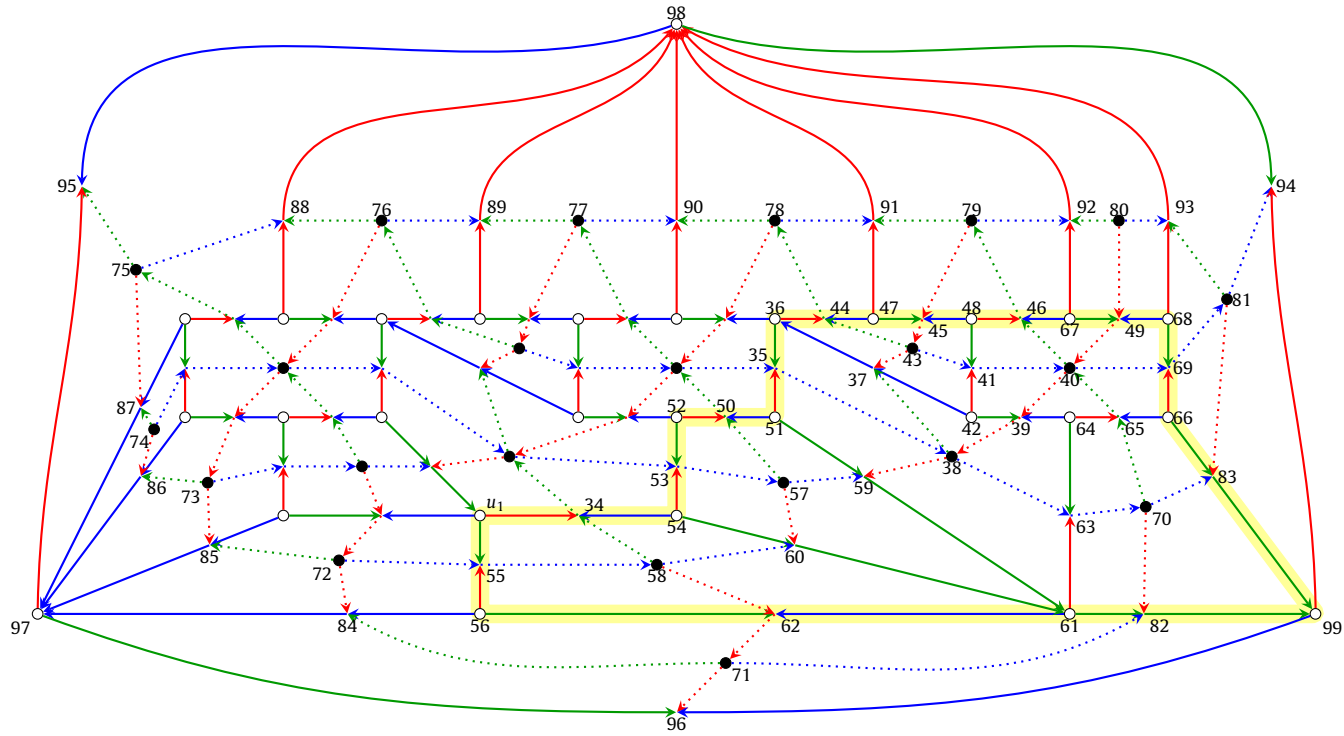


Fig. 25. The completion of the graph G_2 , and its Schnyder wood S_2 . Some vertices and edges in the outer face of G_2 are suppressed to enhance readability. The graph H is encircled in yellow. Part of an elimination order, as in the proof of Theorem 26, is given.

Since $|V(G_k)| = 10k + 8$ we have that

$$\frac{|\{v \mid v \text{ is a singleton in } \mathcal{P}_k^{i,i+1}\}|}{|V(G_k)|} \rightarrow \frac{1}{5}, \text{ for } k \rightarrow \infty,$$

for any choice of $i \in \{1, 2, 3\}$.

Now, we count the number of leaves. We explicitly count the leaves of one tree, namely T_2^k . The number of leaves of T_1^k and T_3^k follows by similar arguments. In G_k only some vertices have more than one ingoing 2-colored edge. Those are the following. The vertex u_1 has two ingoing 2-colored edges. For $i = \{2, \dots, k-1\}$, u_i has three ingoing 2-colored edges. And w_k and r_2 have four ingoing 2-colored edges each. As in the proof of Theorem 22, we obtain that T_2^k has $2k + 4$ leaves. With similar arguments, one can show that the number of leaves in the other two trees is also $2k + 4$. We obtain that for every $j \in \{1, 2, 3\}$

$$\frac{|\{v \mid v \text{ is a leaf in } T_j^k\}|}{|V(G_k)|} = \frac{2k + 4}{10k + 8} \rightarrow \frac{1}{5}, \text{ for } k \rightarrow \infty. \quad \square$$

5. Conclusion

For 3-connected planar graphs, we gave tight lower bounds of the number of singletons in compatible ordered path partitions and of leaves of Schnyder woods. For two of those bounds (Theorem 15 and 22), we additionally know that the respective Schnyder wood is the minimal one. It is somewhat surprising that our bound on the number of singletons (Theorem 15) and our bound on the number of leaves (Theorem 15) almost coincide. This might suggest that there may be an unknown relation linking these two bounds.

In Theorem 20, we gave a slightly better bound on the number of singletons. In exchange, we need to acquiesce that the respective Schnyder wood might not be the minimal Schnyder wood anymore. We conjecture that this also holds for the number of leaves.

Declaration of competing interest

The authors declare that they have no known competing financial interests or personal relationships that could have appeared to influence the work reported in this paper.

Data availability

No data was used for the research described in the article.

References

- [1] M.J. Alam, W. Evans, S.G. Kobourov, S. Pupyrev, J. Toeniskoetter, T. Ueckerdt, Contact representations of graphs in 3D, in: Proceedings of the 14th International Symposium on Algorithms and Data Structures (WADS '15), in: Lecture Notes in Computer Science, vol. 9214, 2015, pp. 14–27, technical Report accessible on arXiv:1501.00304.
- [2] M. Badent, U. Brandes, S. Cornelsen, More canonical ordering, *J. Graph Algorithms Appl.* 15 (1) (2011) 97–126.
- [3] N. Bonichon, B. Le Saëc, M. Mosbah, Wagner's theorem on realizers, in: Proceedings of the 45th International Colloquium on Automata, Languages and Programming (ICALP'02), in: Lecture Notes in Comput. Sci., vol. 2380, Springer, Berlin, 2002, pp. 1043–1053.
- [4] N. Bonichon, C. Gavoille, N. Hanusse, An information-theoretic upper bound of planar graphs using triangulation, in: Proceedings of the 20th Annual Symposium on Theoretical Aspects of Computer Science Berlin, Germany (STACS'03), Springer, 2003, pp. 499–510.
- [5] H. de Fraysseix, J. Pach, R. Pollack, Small sets supporting Fáry embeddings of planar graphs, in: Proceedings of the 20th Annual ACM Symposium on Theory of Computing (STOC'88), ACM Press, 1988, pp. 426–433.
- [6] H. De Fraysseix, J. Pach, R. Pollack, How to draw a planar graph on a grid, *Combinatorica* 10 (1990) 41–51, <https://doi.org/10.1007/BF02122694>.
- [7] P.O. de Mendez, Orientations bipolaires, Ph.D. thesis, École des Hautes Études en Sciences Sociales, Paris, 1994.
- [8] G. Di Battista, R. Tamassia, L. Vismara, Output-sensitive reporting of disjoint paths, *Algorithmica* 23 (4) (1999) 302–340, <https://doi.org/10.1007/PL00009264>.
- [9] E. Di Giacomo, G. Liotta, T. Mchedlidze, Lower and upper bounds for long induced paths in 3-connected planar graphs, *Theor. Comput. Sci.* 636 (2016) 47–55, <https://doi.org/10.1016/j.tcs.2016.04.034>.
- [10] S. Felsner, Convex drawings of planar graphs and the order dimension of 3-polytopes, *Order* 18 (1) (2001) 19–37, <https://doi.org/10.1023/A:1010604726900>.
- [11] S. Felsner, Geometric Graphs and Arrangements, Advanced Lectures in Mathematics, Vieweg+Teubner, Wiesbaden, 2004.
- [12] S. Felsner, Lattice structures from planar graphs, *Electron. J. Comb.* 11 (1) (2004) R15.
- [13] Éric Fusy, Combinatorics of planar maps and algorithmic applications (Combinatoire des cartes planaires et applications algorithmiques), Ph.D. thesis, École Polytechnique, Palaiseau, France, 2007, <https://tel.archives-ouvertes.fr/pastel-00002931>.
- [14] G. Kant, Drawing planar graphs using the lmc-ordering, in: Proceedings of the 33rd Annual Symposium on Foundations of Computer Science (FOCS'92), 1992, pp. 101–110.
- [15] G. Kant, Drawing planar graphs using the canonical ordering, *Algorithmica* 16 (1) (1996) 4–32, <https://doi.org/10.1007/BF02086606>.
- [16] P. Kindermann, T. Mchedlidze, T. Schneck, A. Symvonis, Drawing planar graphs with few segments on a polynomial grid, in: Proceedings of the 27th International Symposium on Graph Drawing and Network Visualization (GD'19), in: Lecture Notes in Comput. Sci., vol. 11904, Springer, Cham, 2019, pp. 416–429.

- [17] C. Ortlieb, J.M. Schmidt, Toward Grünbaum's conjecture, in: 19th Scandinavian Symposium and Workshops on Algorithm Theory, SWAT 2024, June 12-14, 2024, Helsinki, Finland, in: LIPIcs, vol. 294, Schloss Dagstuhl - Leibniz-Zentrum für Informatik, 2024, pp. 37:1–37:17.
- [18] W. Schnyder, Embedding planar graphs on the grid, in: Proceedings of the 1st Annual ACM-SIAM Symposium on Discrete Algorithms, 1990, pp. 138–148.
- [19] H. Zhang, X. He, Compact visibility representation and straight-line grid embedding of plane graphs, in: Proceedings of the 8th International Workshop on Algorithms and Data Structures (WADS'03), in: Lecture Notes in Comput. Sci., vol. 2748, Springer, Berlin, 2003, pp. 493–504.
- [20] H. Zhang, X. He, Optimal st-orientations for plane triangulations, *J. Comb. Optim.* 17 (4) (2009) 367–377.